AD/A-000 538

CHEMICAL STRUCTURAL AGING EFFECTS

George E. Myers

Lockheed Propulsion Company

REPORT DOCUMENTATION PAGE		READ INSTRUCTIONS BEFORE COMPLETING FORM
1. REPORT NUMBER AFRPL-TR-74-58	2. GOVT ACCESSION NO.	3. RECIPIENT'S CATALOG NUMBER AD/A-000 538
4. TITLE (and Subtitle) Chemical Structural Aging Effects		5. TYPE OF REPORT & PERIOD COVERED Final June 1971 - June 1974
		6. PERFORMING ORG. REPORT NUMBER 569-F
7. AUTHOR(s) George E. Myers		8. CONTRACT OR GRANT NUMBER(s) F04611-71-C-0025
9. PERFORMING ORGANIZATION NAME AND ADDRESS Lockheed Propulsion Company P. O. Box 111 Redlands, California 92373		10. PROGRAM ELEMENT, PROJECT, TASK AREA & WORK UNIT NUMBERS
11. CONTROLLING OFFICE NAME AND ADDRESS Air Force Rocket Propulsion Laboratory Edwards, California 93523		12. REPORT DATE October 1974
		13. NUMBER OF PAGES 82
14. MONITORING AGENCY NAME & ADDRESS(if different from Controlling Office) Same		15. SECURITY CLASS. (of this report) Unclassified
		15a. DECLASSIFICATION/DOWNGRADING SCHEDULE

16. DISTRIBUTION STATEMENT (of this Report)

Approved For Public Release: Distribution Unlimited

17. DISTRIBUTION STATEMENT (of the abstract entered in Block 20, if different from Report)

18. SUPPLEMENTARY NOTES

N/A

19. KEY WORDS (Continue on reverse side if necessary and identify by block number)

Minuteman propellant
Accelerated surveillance
Chemical aging
Service life prediction

20. ABSTRACT (Continue on reverse side if necessary and identify by block number)

Aging studies have been conducted upon one batch of ANB-3066 propellant for the purpose of establishing the utility of accelerated surveillance in predicting service life of Third Stage Minuteman. Chemical analyses and physical property measurements were performed during aging at 30 to 145°F and at 0 and 5 percent strain over a period of 120 weeks.

DD FORM, JAN 73 1473   EDITION OF 1 NOV 65 IS OBSOLETE

No measurable changes in functional group concentrations were observed by infrared, and the large increases in crosslinking occurring during aging are therefore believed due to AP oxidative attack upon the polybutadiene backbone. Below 115°F the changes in physical properties, e.g., increasing gel content and decreasing compliance, could be described by equations which were linear in logarithmic time. At 145°F, evidence was found for a reversion in the initial hardening after approximately 15 weeks, necessitating the addition of a quadratic term in logarithmic time. Temperature dependence of the rate constants followed the Arrhenius equation.

Good agreement was observed between available long-term (6 to 7 years) 80°F aging data and the extrapolated prediction of the 70°F aging equation from this program. However, shorter term data (2 years) for additional batches demonstrated pronounced batch-to-batch variations in aging behavior. Predicted service lives decreased strongly with temperature (~ factor of 10 from 70 to 145°F) and also with aging under strain (~ factor of 2 at 70°F between 0 and 5 percent strain).

Thus, empirical correlations can indeed be employed which will allow the use of accelerated surveillance to predict chemical aging rates of ANB-3066 under silo storage conditions. However, batch variations may be significant, and the use of stress-free carton aging data may strongly overestimate the useful life of propellant within a motor grain.

<div style="text-align: center;">NOTICES</div>

<div style="text-align: center;">FOREWORD</div>

This is the final report issued under Contract F04611-71-C-0025, "Chemical Structural Aging Effects", a program conducted by Lockheed Propulsion Company, Redlands, California, and monitored by the Air Force Rocket Propulsion Laboratory (Robert A. Biggers, MKPB). Participating technical personnel were Dr. W. E. Baumgartner (Chemistry Department Manager), Dr. G. E. Myers (Program Manager), Dr. A. B. Tipton (Project Engineer), Mr. G. Horstman, and Mr. W. G. Stapleton. Dr. H. A. Leeming of Leeming Associates, Dr. W. Knauss of Cal Tech, and Mr. D. Kaelble of North American Rockwell served as technical consultants to the program.

This report contains no classified information.

This report has been reviewed and approved.

FOR THE COMMANDER

CHARLES R. COOKE, Chief
Solid Rocket Division

iii

TABLE OF CONTENTS

TABLE OF CONTENTS (Continued)

NOTICES

FOREWORD

This is the final report issued under Contract F04611-71-C-0025, "Chemical Structural Aging Effects", a program conducted by Lockheed Propulsion Company, Redlands, California. and monitored by the Air Force Rocket Propulsion Laboratory (Robert A. Biggers, MKPB). Participating technical personnel were Dr. W. E. Baumgartner (Chemistry Department Manager), Dr. G. E. Myers (Program Manager), Dr. A. B. Tipton (Project Engineer), Mr. G. Horstman, and Mr. W. G. Stapleton. Dr. H. A. Leeming of Leeming Associates, Dr. W. Knauss of Cal Tech, and Mr. D. Kaelble of North American Rockwell served as technical consultants to the program.

This report contains no classified information.

This report has been reviewed and approved.

FOR THE COMMANDER

CHARLES R. COOKE, Chief
Solid Rocket Division

LIST OF ILLUSTRATIONS

AFRPL-TR-74-58

LIST OF ILLUSTRATIONS (Continued)

LIST OF TABLES

(The reverse is blank)

1. INTRODUCTION

1.1 PROGRAM OBJECTIVES

Reliable assessment of service life is assuming increasing importance as the concept of "life cycle cost" is increasingly recognized to be one of the overriding criteria in system selection. The specific object: of this program was to establish whether, and to define how, accelerated surveillance could be employed to predict the service life of Minuteman Third Stage (ANB-3066) propellant stored under silo conditions (70±10°F). Development of such capability obviously has much broader implications in terms of its application to prediction of phase-out or replacement rates for other existing missile systems and also in terms of its application to the evaluation of true potential of propellant systems during their development.

1.2 THE GENERAL PROBLEM OF SERVICE LIFE PREDICTION

1.2.1 Chemical Aging and Fatigue

In the most general and proper sense the service life of propellant in an actual motor grain is controlled by two processes which are not necessarily independent and at times indeed may be inseparable. These two processes are chemical aging and fatigue.

We define chemical aging as those changes in propellant properties which result from chemical reactions occurring after completion of the normal cure cycle. Those reactions can be extremely complex in a solid propellant but for ANB-3066 (Butarez-CT/HX-868) might be expected to include such processes as: continued reaction between residual carboxy and imine groups, reaction between carbonyl and oxazoline, homopolymerization of HX-868, free radical reactions involving polybutadiene segments and O_2 or AP, thermal degradation, hydrolysis.

Fatigue, on the other hand, we define as a degradation in ability to withstand loads as a consequence of previous loading, in effect a cumulative damage. Fatigue failure is generally regarded as arising from microscopic flaws or structural inhomogeneities which lead to macroscopic cracks and ultimate rupture under imposed stress. Since there will always be a distribution of flaw sizes (and/or localized stress intensities), fatigue failure is inherently a statistical process and results in a very wide distribution of failure times.

Methods of predicting service life solely from the point of view of fatigue, i.e., ignoring chemical aging, have included the reaction kinetics approach (Ref. 1) and the Aerojet cumulative damage approach (Ref. 2). More recently, LPC has demonstrated promise (Ref. 3) in an approach involving an extension of the Halpin-Polley description of the statistics of constant load fatigue failure for plastics (Ref. 4). In effect the distribution of failure times is described by so-called Weibull statistics, i.e.,

$$\frac{N(t)}{N_o} = \exp - \left[\frac{kt}{a_T \, a_\sigma} \right]^n \tag{1-1}$$

where $N(t)$ is the number of samples survived after time t, N_o is the original number of samples, k is a rate (time scale) parameter, n is a parameter characterizing the type of distribution, and a_T and a_σ are temperature and load shift factors.

The structural change accompanying or underlying fatigue damage might be considered physical in nature, e.g., creep or physical desorption of binder from filler. However, it is difficult to imagine other micro-structural changes during fatigue which will not entail chemical changes of some sort, e.g., chain scission at the leading edge of a growing flaw. It is recognized, moreover, that the presence of a stress field may significantly enhance the rates of chemical reactions by virtue of the fact that the strain energy introduced into various chemical bonds will effectively reduce the activation energy required for reaction; this notion has been formalized in the so-called Zhurkov rate equation

$$K = K_o \exp \left[\frac{-E + \gamma \sigma}{RT} \right] \tag{1-2}$$

where E is the normal thermal activation energy and γ is a factor characterizing the effectiveness of imposed stress σ in altering the reaction rate.

Thus the boundary between chemical aging and fatigue is a diffuse one. Furthermore, the structural changes brought about by strictly chemical aging processes will greatly alter the ability of the propellant to resist fatigue damage, in terms of both the shape of the failure distribution and of orders of magnitude changes in average time to failure. This is graphically illustrated by the following values for gel content and fatigue rate constant (k in equation 1-1) obtained by LPC on aged TP-H1011 propellant:

Gel Content (%)	Fatigue Rate Constant
42.2	2.5×10^{-1}
45.0	4.0×10^{-3}
47.6	1.5×10^{-4}

We come, therefore, to the crux of the problem. A complete service life prediction for a propellant grain must ultimately be able to account quantitatively for the effects of chemical aging upon the propellant's fatigue

resistance. This implies that the following are quantitatively describable as a function of aging time under realistic service conditions (temperature, stress, environment):

- The statistical distribution function of failure times under loading conditions which represent the known failure modes of the system, e.g., bore cracking during thermal cycling or ignition.

- The rate of change, due to chemical aging, of the parameters of the statistical distribution function, e.g., k, n, a_σ, a_T of equation (1-1). It should be noted that this must include any influence of grain internal stress upon chemical aging rates.

1.2.2 Accelerated Surveillance

The problem of developing reliable service life predictability is aggravated further by the desire for long-term visibility. This necessitates the use of accelerated surveillance and consequent extrapolations in time/temperature/load/environment as appropriate.

In the simplest and by far the most usual case, surveillance is carried out on propellant cartons at several elevated temperatures plus the actual service temperature. At intervals during aging (short term relative to anticipated lifetime) physical tests are run which provide parameters believed to be critical with regard to the actual failure mode. Attempts are then made to perform temperature/time extrapolations of the data to establish the time at service temperature when the critical parameter reaches its limiting permitted value.

In general such usage of accelerated surveillance data has met with limited success and at the initiation of this program there appeared to be three reasons for this:

(1) The presumed complexity of the chemical changes taking place made it unlikely that a single activation energy would be applicable over the temperature range of interest. Thus, a simple temperature extrapolation of an overall rate of change would be invalid, as illustrated in Figure 1-1.

(2) Each chemical process might be expected to exert a different quantitative effect upon a given propellant mechanical property, as illustrated in Figure 1-2.

(3) Rate acceleration can also be brought about by the stress fields within the propellant grain of an actual motor (see equation 1-2). Rates of property change measured upon unstressed cartons, therefore, may not accurately reflect rates of change occurring in a motor grain.
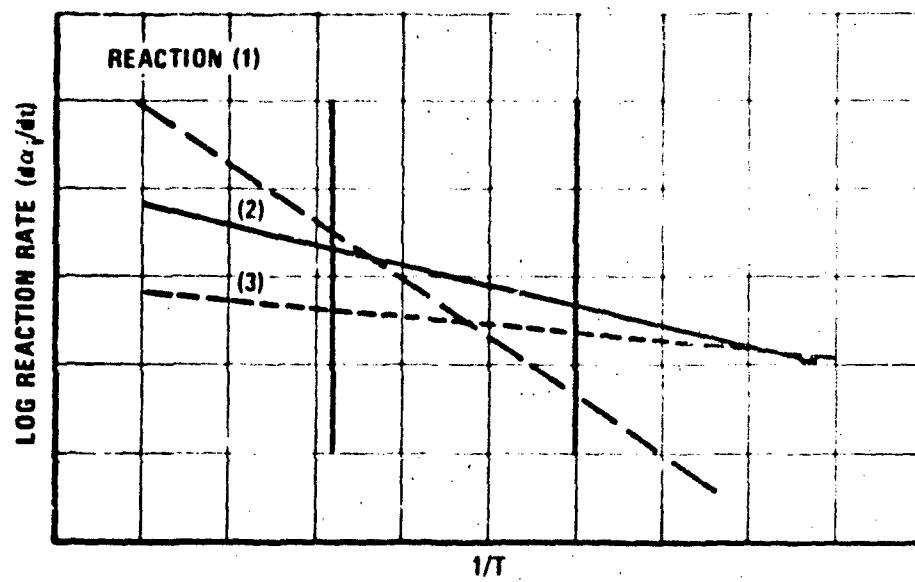
Figure 1-1   Schematic Illustration of Complexity of Reactions in Propellant
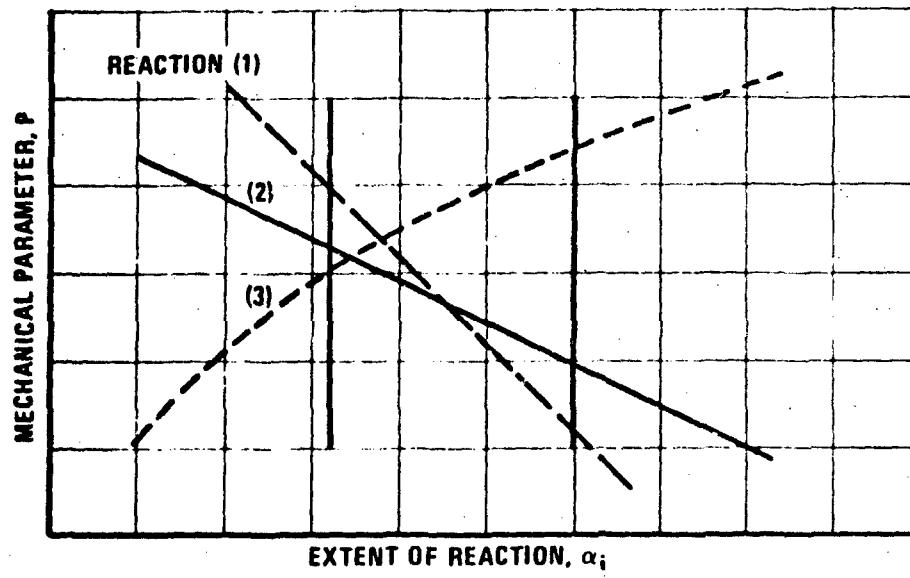
Figure 1-2   Schematic Illustration of Dependence of Mechanical
Parameters Upon Various Reactions in Propellant

1.3 PROGRAM GOALS, SCOPE, AND APPROACH

The above discussion demonstrates that the problem of service life prediction is many-faceted and difficult. This program examined primarily one facet, the question of how best to use elevated temperature surveillance data to predict chemical aging-controlled service life of ANB-3066 propellant. Fatigue and its associated failure statistics were ignored. However, the possible acceleration of chemical aging was investigated by comparing, throughout the program, rates of change in unstressed samples with those held under constant strain.

As originally established, this program (and the parallel program conducted by Thiokol on TP-H1011 propellant) intended to achieve its goal of making accelerated surveillance meaningful by: (1) identifying the controlling chemical reactions at the various temperatures, (2) quantifying their rates and temperature coefficients, (3) defining their relationships to simultaneous rates of change in particular physical parameters. By achieving such an understanding it was expected that rational procedures for temperature/time extrapolation could be defined and valid service life predictions (based upon chemical aging) could be obtained.

At the outset, therefore, a number of chemical and physical tests were performed upon aging ANB-3066 propellant (strained and unstrained) and upon propellant analogs. It became apparent, however, that although the physical/mechanical changes induced by chemical aging were quite large, the underlying changes in concentration for the various chemical moieties (carboxyl, amide, ester, C=C) were small. In fact it appeared that such changes were, for the most part, hidden within the data scatter and that more extensive method development would be necessary to achieve quantitative definition of rates of chemical reactions during aging. Emphasis was thereafter placed upon defining quantitative rates of change for selected physical/mechanical parameters and establishing a rationale for correlating such data and performing temperature/time extrapolations.

The program therefore involved the following specific tasks:

(1) ANB-3066 propellant was procured from Thiokol as one-gallon cartons which were prepared from one 300-gallon batch using Minuteman production facilities and specifications (see Appendix A). A KCl ana og propellant (KCl replacing AP) was prepared at LPC in a 1 gallon batch.

(2) The primary conditions of storage of ANB-3066 are listed in Table 1-1, additional details being given in Appendix A. A few samples were also aged at 3 percent constant strain or at approximately 10 psi stress. The 30^0F storage served as a propellant "bank" from which samples could be removed for initiation of higher temperature aging as desired. A limited number of cartons of the KCl analog propellant were aged at 0 to 3-percent strain.

(3) Physical and chemical tests were performed upon the propellant at intervals during an approximately 120-week period. The primary tests included infrared, gel content, creep compliance (at -40 and +100°F), dilatation, crack propagation (see Appendix A for details).

(4) The physical/mechanical property data were analyzed and methods developed to permit temp   ure/time extrapolations of observed changes and provide   vice life predictions based upon chemical aging.

Table 1-1

AGING CONDITIONS[a]

Temperature (°F)	Strain (%)	Total Elapsed Time (Weeks, Nominal)
30	0	91
70	0 and 5	121
86	0 and 5	68
115	0 and 5	121
145	0 and 5	87

[a] Aged as blocks (~4" x 4" x 5") in N_2-purged, sealed cans.

2. SUMMARY

An investigation has been conducted into the <u>chemical</u> aging of ANB-3066 Minuteman propellant for the purpose of establishing means to employ accelerated surveillance data for predicting useful life under silo storage conditions (70 ± 10^0F, inert atmosphere).

To this end a propellant batch was procured from Thiokol which was prepared according to Minuteman specifications. Cartons of this propellant were aged under N_2 at 30, 70, 86, 115, and 145^0F and at 0 and 5 percent constant strain for periods up to 120 weeks. At intervals during aging, chemical analyses (primarily infrared) were performed and physical tests were conducted, the latter consisting of gel content, degree of swell, creep compliance (-40 and $+100^0$F), dilatation, and crack propagation. The resulting data were analyzed and correlated to establish their utility for prediction of chemical aging - controlled service life. The findings of this study are summarized in the following subsections.

2.1 CHEMICAL STUDIES AND AGING MECHANISM

Infrared measurements demonstrated that carboxyl groups remained after cure and did not measurably decrease during long-term aging. Wet analyses by Thiokol are consistent with this finding and indicate, moreover, that $C=C$ double bond content decreases with aging.

Since the propellant exhibits strong increr es in gel content and in modulus during aging, it is postulated that interchain crosslinking occurs through AP oxidative attack adjacent to $C=C$ positions. LPC data indicate that a reversion process also becomes important at high temperatures (145^0F), after an initial period of hardening, and leads to subsequent softening. That reversion process perhaps is the consequence of a changing balance in oxidative crosslinking/scission and/or of hydrolysis by the water produced from oxidative reactions.

Dilatation appears to decrease while binder modulus (gel content) increases and compliance decreases. These contrasting effects may indicate that increased crosslinking of "bulk" binder is accompanied by improvement in the binder/filler bonding and/or interfacial structure.

2.2 ANALYSIS OF AGING RATES OF PHYSICAL PROPERTIES

Changes in physical properties during aging were described as the following functions of logarithmic time:

$$P = P^0 + k \log t \qquad\qquad (2-1)$$

$$P = P^0 + k_1 \log t + k_2 (\log t)^2 \qquad\qquad (2-2)$$

where P and P^0 are the values of the property at time t and at time $t = 1$ week respectively and the k's are aging rate constants.

At all aging conditions except $145°F$ after about 15 weeks, the quadratic equation generally was not statistically superior to the linear equation. At $145°F$ after about 15 weeks, however, it became necessary to employ the quadratic equation with k_1 and k_2 of opposite sign, i.e., a reversion of the initial hardening was indicated.

Comparison of the aging data for this batch of ANB-3066 propellant with data available for other batches demonstrated that strong batch-to-batch variations in aging behavior can exist, particularly at higher temperatures. Such variations are not unexpected since small changes in effective stoichiometry and/or cure cycle can move the propellant binder structure back onto the steep portion of the gel/extent of reaction curve. Only the LPC high-temperature data gave strong indication of a reversion at longer aging times, although other batches did appear to be approaching a steady state. While differences in behavior were noted at 70 to $80°F$, extrapolation of LPC's linear regression equation for compliance (based upon 120-week aging data) showed very satisfactory agreement with long-term (7 to 8 years) modulus data for a single batch by Aerojet and for numerous batches (single point each) by Hill Air Force Base.

Where the data were sufficiently extensive to provide reliable values of the rate constants (k, k_1, k_2), their temperature dependence could be described by an Arrhenius approach, i.e.,

$$K (=k, k_1, k_2) = K^0 \exp\left[\frac{-B}{RT}\right]. \qquad\qquad (2-3)$$

For k and k_1, the apparent activation energy (B) was quite small (2-3 kcal/mole for k), consistent with a diffusion control of the crosslinking process and/or a free radical reaction. The value of B for k_2 was several-fold greater; however, the significance of this is not clear due to the relatively large error in determining k_2.

Aging under 5 percent strain increased both the rate of aging from 70 to $145°F$ and the apparent activation energy. For example, the k values for compliance after strained/unstrained aging were -0.75/-0.68 and -1.45/-1.08 at 70 and $145°F$, respectively, and the B values were 2.8/2.0. Although the rate increase caused by aging under 5 percent strain was only 10 percent at $70°F$, this can have a major effect on the predicted service life due to the logarithmic time dependence.

The observed rate constants were employed to extrapolate calculated aging curves for compliance to an approximated failure criterion, thus yielding predicted chemical aging-controlled service lives. Using a ± one σ error in both the failure criterion and the calculated aging curves, the predicted service life at 70°F, 0-percent strain is between 4.6 and 11 years. Assuming that the relative standard deviation of regression for the compliance curve were to be decreased from the observed value of 3.4 percent to a value of 1 percent, the predicted useful life would become 5.8 to 9.6 years. The effect of a reversion process, or of achieving a steady state, can be to increase the service life significantly. The effect of aging under 5 percent strain is to reduce the predicted minimum life at 70°F by approximately a factor of two.

2.3 CONCLUSIONS AND RECOMMENDATIONS

The conclusions of the program and the consequent recommendations are discussed in Section 4 of this report. They may be outlined briefly as follows:

(1) Accelerated surveillance data for ANB-3066 can be empirically correlated to permit time and temperature extrapolations and thereby provide silo service life predictions based upon chemical aging rates.

(2) The observed hardening of ANB-3066 apparently is not caused by continued reaction between the rather large quantities of residual carboxyl and imine. Instead, it is probably the consequence of crosslinking reactions involving AP oxidative attack upon polybutadiene backbone double bonds.

(3) Aging under 5 percent constant strain increases aging rates and reduces the predicted service life. Therefore, the use of surveillance data obtained upon isolated propellant cartons may yield too optimistic service life predictions for actual motor grains. It should be noted further that this program has not considered any other interactions between chemical aging and mechanical forces, such as the effect of changing stress fields (temperature changes, vibration) upon chemical aging rates or the effect of chemical aging upon fatigue resistance.

(4) Significant gains in service life might be gained by storage at temperatures below 70°F, where rates of hardening would be lower, or by storage above 70°F, where possible reversion rates would be faster.

(5) Batch-to-batch variations in aging rate and pattern exist and render generalization of quantitative predictions from one batch questionable. The equations employed in this study to correlate and extrapolate the data should be regarded as empirical, and other relations should be considered for other ANB-3066 batches and for other propellants. Reliability of service life predictions would be greatly enhanced by instituting tighter quality control limits and control procedures (e.g. gel content measurement) which are informative as to the state of cure and the initial course of aging.

(6) Large uncertainties in predicted service life may be introduced by relatively small errors in aging rates, the latter occasioned by errors in property measurements and by propellant inhomogeneity. Surveillance programs, therefore, should concentrate upon a very small number of parameters whose aging changes can be measured reproducibly over a broad temperature/time regime.

3. RESULTS AND DISCUSSION

3.1 CHEMICAL STUDIES AND AGING MECHANISM

During the initial portion of the program several different chemical techniques were applied to the aging ANB-3066 and to the KCl analog to determine their usefulness for clarifying the aging mechanism and the effects of mechanical loading thereon. Some preliminary results of gas evolution analyses and of examination of sol extracts by GPC and infrared, for example, were reported earlier (Ref. 5): such experiments were not continued since it was judged that they would be only of indirect value to quantitative aging predictions.

During the course of the program a variety of infrared experiments was also conducted. As experiments progressed, significant improvements in technique and apparatus evolved, but the resultant data differences made it difficult to define long-term chemical changes in quantitative terms. Because of this and the small changes observed in concentration of the various structural moieties during aging, the infrared data obtained could be used only qualitatively.

Initial screening experiments involved a comparison of the cure (110^0F) and aging (145^0F) of the Butarez/HX-868 binder relative to the same binder in contact with AP. Two multiple internal reflectance (MIR) infrared cells were used, one with binder only and one with a very thin layer of binder in contact with a pressed AP tablet.* Reactions involving the carboxyl/imine curative linkage were followed using the C=0 stretch bands of the acid (1720 cm^{-1}) and ester (1740 cm^{-1}) and the amide II band (1540 cm^{-1}). Figure 3-1 shows the absorbances of these bands normalized by that of the methylene C-H stretch band (2845 cm^{-1}, and plotted against cure and aging time. These results indicate the following:

- The carboxyl groups are only 30 to 50-percent reacted at end of cure.

- Little if any change in carboxyl, ester, or amide II occurs between end of cure and 5 weeks aging at 145^0F (the imine band virtually disappears during cure).

- No pronounced difference between pure binder and interfacial binder appears.

---

* The binder layer was made sufficiently thin so that weak AP bands could be observed.
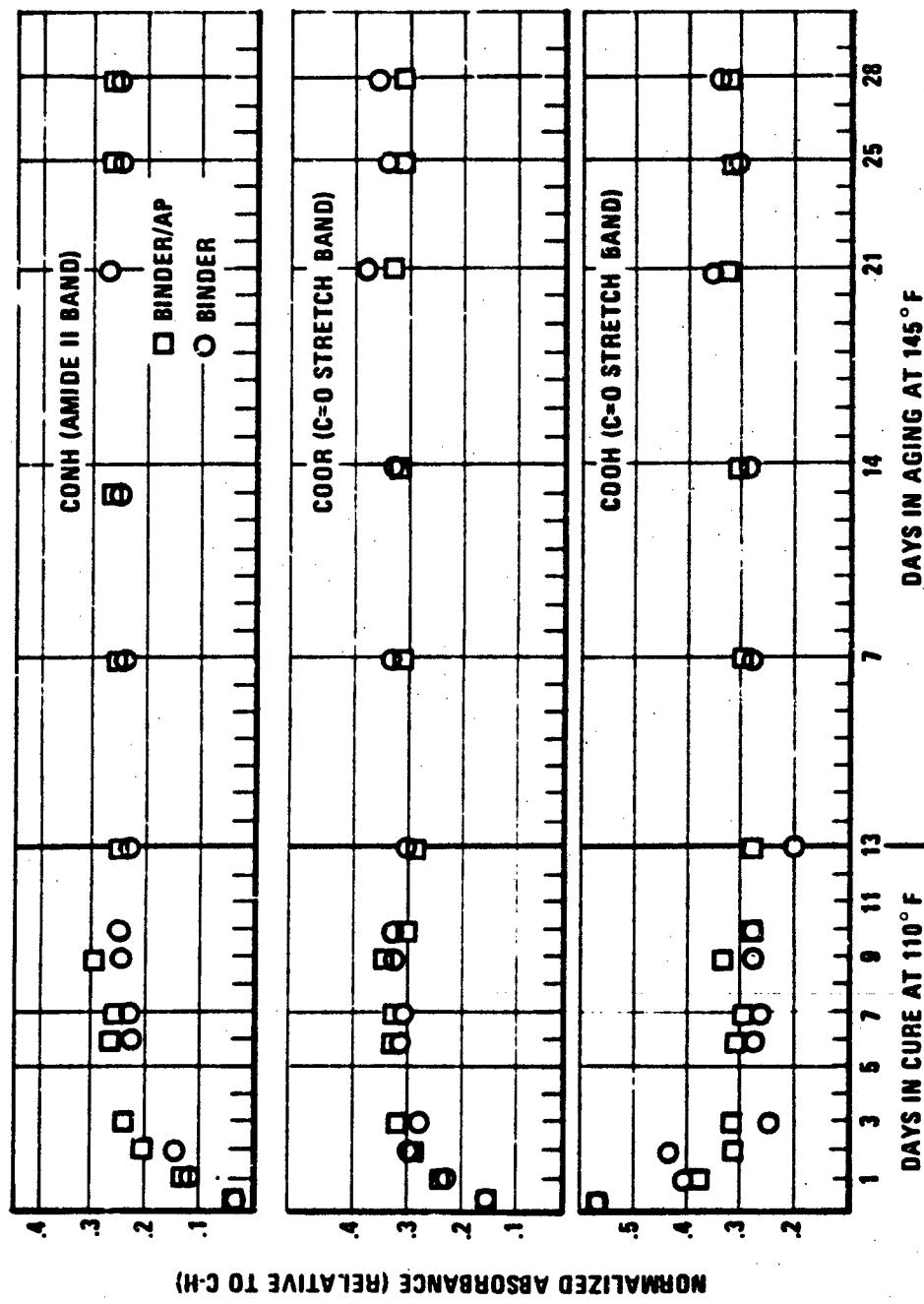
Figure 3-1 MIR Data for Binder and Binder/AP Interface

Results of some reflectance infrared measurements on ANB-3066 propellant and KCl analog are summarized in Table 3-1. These measurements were taken upon thin slices microtomed from the interior of cartons. Since AP absorptions interfere with the amide (1540 cm^{-1}) and also with trans and vinyl C=C bands (960 cm^{-1} and 910 cm^{-1}), only the carboxyl/ester ratio is reported. The initial point for unaged ANB-3066 propellant is believed to be considerably in error since an increase in the COOH/COOR ratio upon early aging is inconsistent with Figure 1-1 and with all expectations. Any other changes in the aging data appear to be within experimental scatter. The lower value of COOH/COOR for the KCl analog is indicative of more complete reaction during cure and this is consistent with its initial gel content of 88 percent compared with less than 60 percent for unaged ANB-3066.

Because of the AP interferences with amide and C=C absorptions, the procedure was modified to permit measurements after extraction of all AP. For this purpose the propellant slices were extracted with $CHCl_3$ and the resultant sol examined by transmittance infrared; the gel was further extracted with pyridine to remove AP and the final dried gel examined by reflectance infrared. Results for the limited number of samples which could be tested are shown in Table 3-2 as ratios of the sol plus gel absorbances. Here again there appear to be no discernible trends upon aging.

Thus, the infrared measurements say that changes in chemical composition during these aging periods are very slight despite the fact that a large fraction of the original carboxyl groups remains unreacted at end of cure. This finding is consistent with wet analyses by Thiokol who report that approximately 24 percent of the original carboxyl and 13 percent of the original imine groups remain after cure of ANB-3066 and are still apparently unreacted after nearly 1 year at $115^\circ F$ (Ref. 6).

Nevertheless, as will become apparent later, major changes in the elastomer structure and mechanical properties are indeed occurring. Qualitatively, the direction of change in various parameters at moderate temperatures and times is indicated in the following:

Gel Content	- Increase
Swell	- Decrease
Compliance	- Decrease
Dilatation (Low Strain)	- Decrease
Critical Stress	- Increase

Except for dilatation these changes all seem to follow logically from the rising binder modulus inherent in increasing gel content. The decrease in tendency toward dilatation, however, appears contradictory to increased binder modulus unless we postulate a simultaneously enhanced bonding between binder and filler and/or formation of a more nearly optimum interfacial structure. The nature of this structure is, of course, not clear and certainly the infrared interfacial measurements in Figure 3-1 do not demonstrate any distinctive chemical changes within the interface during aging which involve the curative linkage moieties.

Table 3-1

PROPELLANT INFRARED DATA

System	Aging Condition			COOH/COOR[2] Absorbance Ratio
	Temperature (^{0}F)	Strain (%)	Weeks[1]	
ANB-3066	Unaged			1.08±0.05
	30	0	50	1.29±0.10
		0	91	1.24±0.07
	86	0	8	1.30±0.07
		5	8	1.33±0.06
		0	22	1.31 --
		0	36	1.26±0.07
	115	0	7	1.31±0.12
		5	7	1.37±0.05
		0	14	1.47±0.07
		5	14	1.33±0.04
		0	22	1.21 --
	145	0	10	1.25±0.10
		0	56	1.34±0.03
		0	77	1.34±0.12
KCl Analog	Unaged			0.91±0.05
	86	0	8	0.86±0.01
		3	8	0.89±0.01

[1] Nominal aging times

[2] A (1720 cm^{-1})/A (1740 cm^{-1}). Errors are standard deviation for at least duplicate scans on duplicate samples. Where no error is given, only a single scan was made.

Table 3-2

INFRARED DATA FOR EXTRACTED PROPELLANT

Aging Condition			Absorbance Ratio			
			Sol + Gel[2]			Propellant
Temperature (^{0}F)	Strain	Weeks[1]	$\dfrac{\text{COOH}}{\text{COOR}}$	$\dfrac{\text{COOR}}{\text{CONH}}$	$\dfrac{\text{Vinyl}}{\text{Trans}}$	$\dfrac{\text{COOH}}{\text{COOR}}$
30	0	77	1.33	0.86	0.84	--
		99	1.31	0.97	0.84	1.24
86	0	22	1.31	0.78	0.89	1.31
		36	1.30	0.86	0.83	1.26
145	0	56	1.23	1.04	0.86	1.34
		77	1.39	0.79	0.89	1.34

---

[1] Nominal aging time

[2] Transmittance on sol (CHCl$_3$ extract) and reflectance on gel remaining after CHCl$_3$ and pyridine extraction. Corrected for fraction of sol and gel in propellant.

It is interesting to speculate that the increased overall crosslink density (higher gel) and the modified interfacial bonding/structure are consequences of an oxidative attack by AP upon the polybutadiene backbone. The vinyl/ trans infrared absorbance ratios in Table 3-2 argue against this insofar as one would expect a change in that ratio to be produced by oxidative attack. On the other hand, Thiokol reports a marked decrease in total C=C concentration during ANB-3066 aging, as judged by iodimetric measurements (Ref. 6). Therefore, intermolecular crosslinking through AP oxidative reaction with the polymer backbone may be inferred.

The reduction in double bond concentration reported by Thiokol is so large, however, that it seems unlikely that for each double bond lost a crosslink is formed. Instead, competitive crosslinking/chain scission processes probably occur, with the balance normally in favor of crosslinking. It will be pointed out later in this report, however, that some of the ANB 3066 aging data strongly indicate a reversion to be taking place at higher temperatures after the initial period of propellant hardening. Perhaps this reversion is also a consequence of AP oxidation due to a change in the crosslinking/ scission balance or to hydrolytic attack by the water produced in oxidation reactions.

3.2   AGING RATES OF PHYSICAL AND MECHANICAL PARAMETERS

3.2.1   Experimental Data and Parameter Cross Correlation

Experimental values of the parameters which were followed during aging of ANB-3066 propellant are tabulated in the Appendix as Tables A-1 through A-6; the experimental methods are described in the text accompanying those tables. Included in the tables is the standard deviation of each measurement, while the overall relative standard deviations for each of the parameters are summarized in Table 3-3. The observed precision for some parameters, e.g., gel, swell, D_1 ($100^\circ F$), is quite good but for others it is quite poor, particularly where the experimental method involves a subjective element as is the case for crack propagation.

Prior to conducting a kinetic analysis of these parameters, their degree of cross-correlation was examined. This was done for several reasons:

●   To clarify the aging mechanism — as discussed earlier.

●   To clarify/justify the possible elimination of any data points from the kinetic analysis.

●   To provide additional guidelines for the selection of preliminary "zero time" values of the parameters, values which were experimentally unavailable due to the delay in receiving the propellant.

Table 3-3

PRECISION OF PHYSICAL/MECHANICAL PARAMETERS

Parameter	Relative Standard Deviation (%)[1]
Gel	1.6
Swell	3.2
D_1 (100°F)	2.3
D_1 (-40°F)	5.8
n (100°F)	5.5
n (-40°F)	10
$\Delta V/V$	14
γ_c	22
τ_c	12
ϵ_c	9
Crack Growth Rate	~20

---

[1] Relative to initial (nominally unaged) value for each parameter.

Figures 3-2 through 3-6 show the correlations of some of the parameters against gel content, the latter chosen because it is the primary structural variable measured and exhibits the best precision. Where it seemed at all warranted, linear regressions were performed, the resultant equations and regression coefficients being given in the figures.

The degree of inter-parameter correlation is relatively poor, the best case being for swell/gel where only 66 percent of the changes in S are explainable by the linear model. Many of the deviations are greater than would be anticipated from the levels of precision given in Table 3-3. This is undoubtedly the consequence of three factors: (1) propellant inhomogeneity, (2) changes in aging mechanism with time (e.g., the highest compliance point in Figure 3-3), and (3) the fact that each parameter may respond in a complex fashion to changes in gel content. Even in the case of swell, for example, the actual measurement may reflect changes in both bulk binder crosslink density and in interfacial structure (permeability to toluene and/or dewettability by toluene). Still, where an appreciable degree of correlation exists (e.g., Figures 3-2, 3-3, 3-4), those data points which deviate the most also deviate most from simple parameter/aging time plots; such data points were regarded with caution in performing kinetic analyses.

3.2.2 Kinetic Analysis of Parameter Aging Changes

A logarithmic time scale provides a natural base for quantitative comparison of short and long-term propellant aging data because it provides simultaneous visibility and because much of the propellant aging data is at least approximately exponential in nature, presumably due to depletion of reactants and increasing diffusional restrictions. However, since there is no obvious reason why the aging behavior should be precisely exponential, the program data were generally analyzed by both of the following equations:

$$P = P^0 + k \log t \qquad\qquad (3-1)$$

$$P = P^0 + k_1 \log t + k_2 (\log t)^2 \qquad\qquad (3-2)$$

where P and P^0 represent the value of an experimental parameter at time t and at time $t=1$ week, respectively, and the k's represent "aging rates".

The choice between equations (3-1) and (3-2) was determined on the basis of conventional analysis of variance; where the latter indicated no statistical preference existed beyond the 70-percent confidence limit, the linear equation (3-1) was chosen. This was a convenient reference point since the confidence limits were generally either above 70 or well below it.

Obviously, more complex empirical expressions might have been selected which would have given statistically more satisfactory data correlation. For example, it was assumed quite arbitrarily that "zero" aging time corresponded to 1 week, independent of aging condition, whereas a truer representation would include a temperature dependent time scale shift factor. This and other complexities seemed unwarranted, however, in view of the

Figure 3-2 Swell Versus Gel
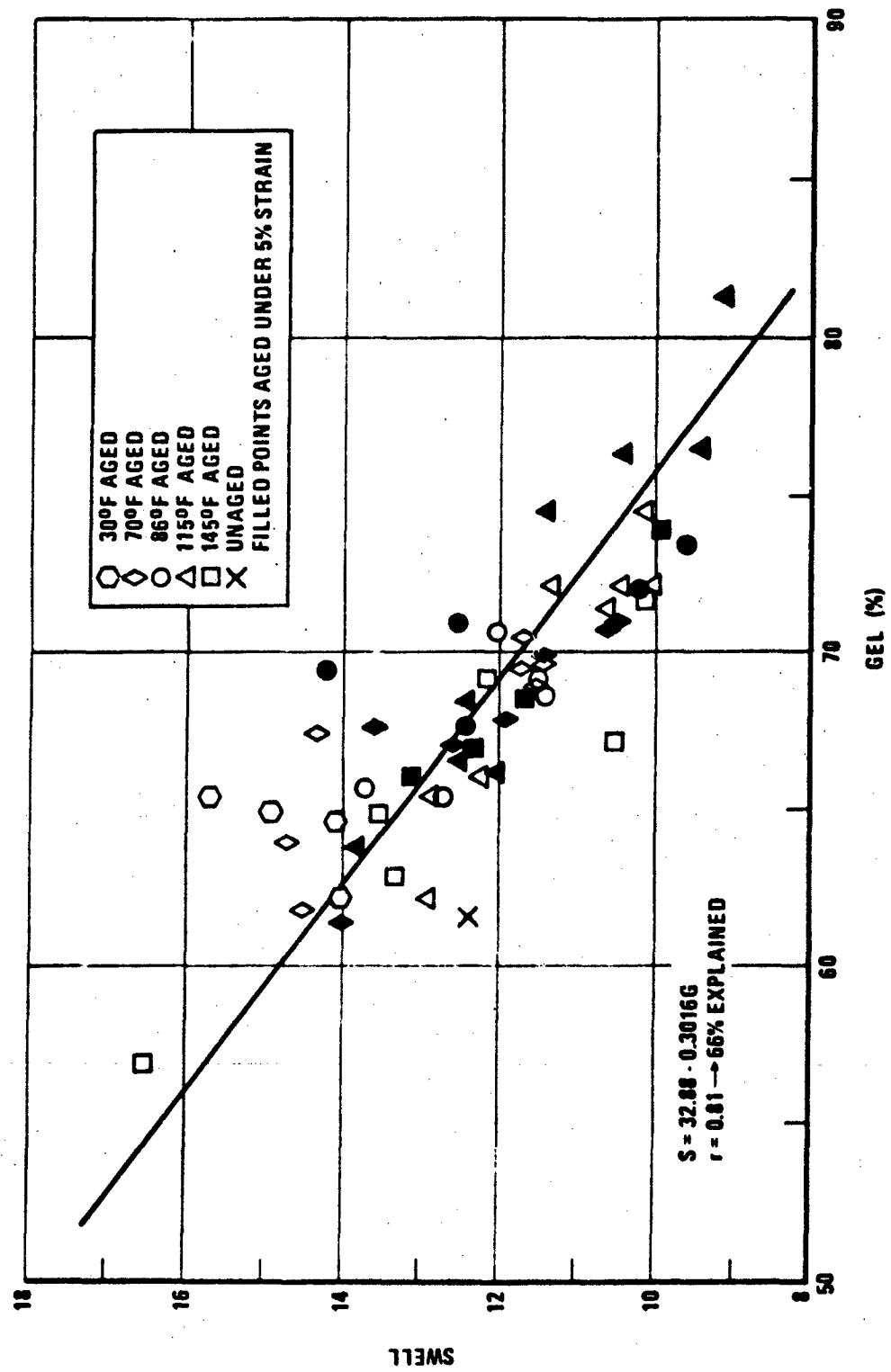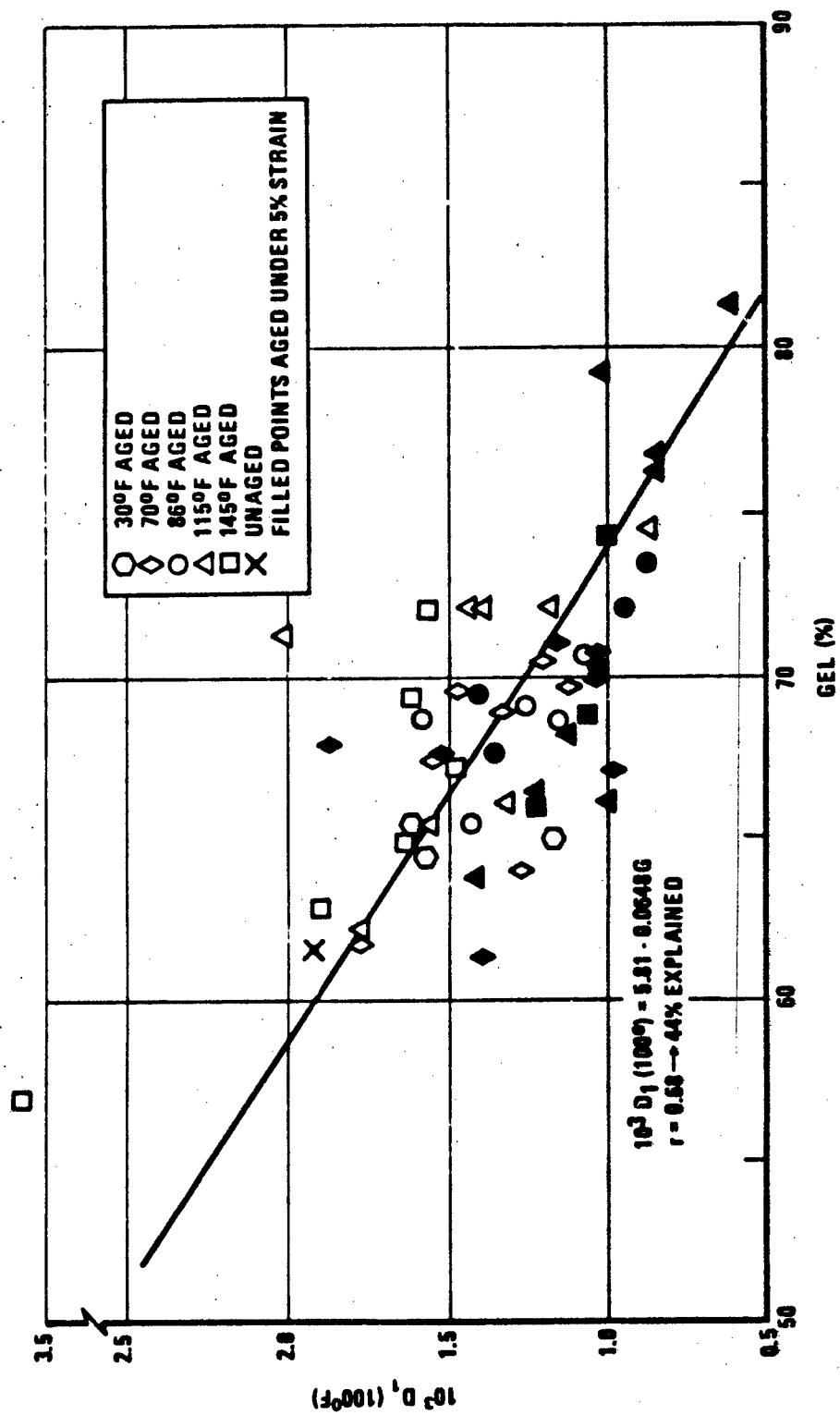
Figure 3-3   Compliance (100°F) Versus Gel
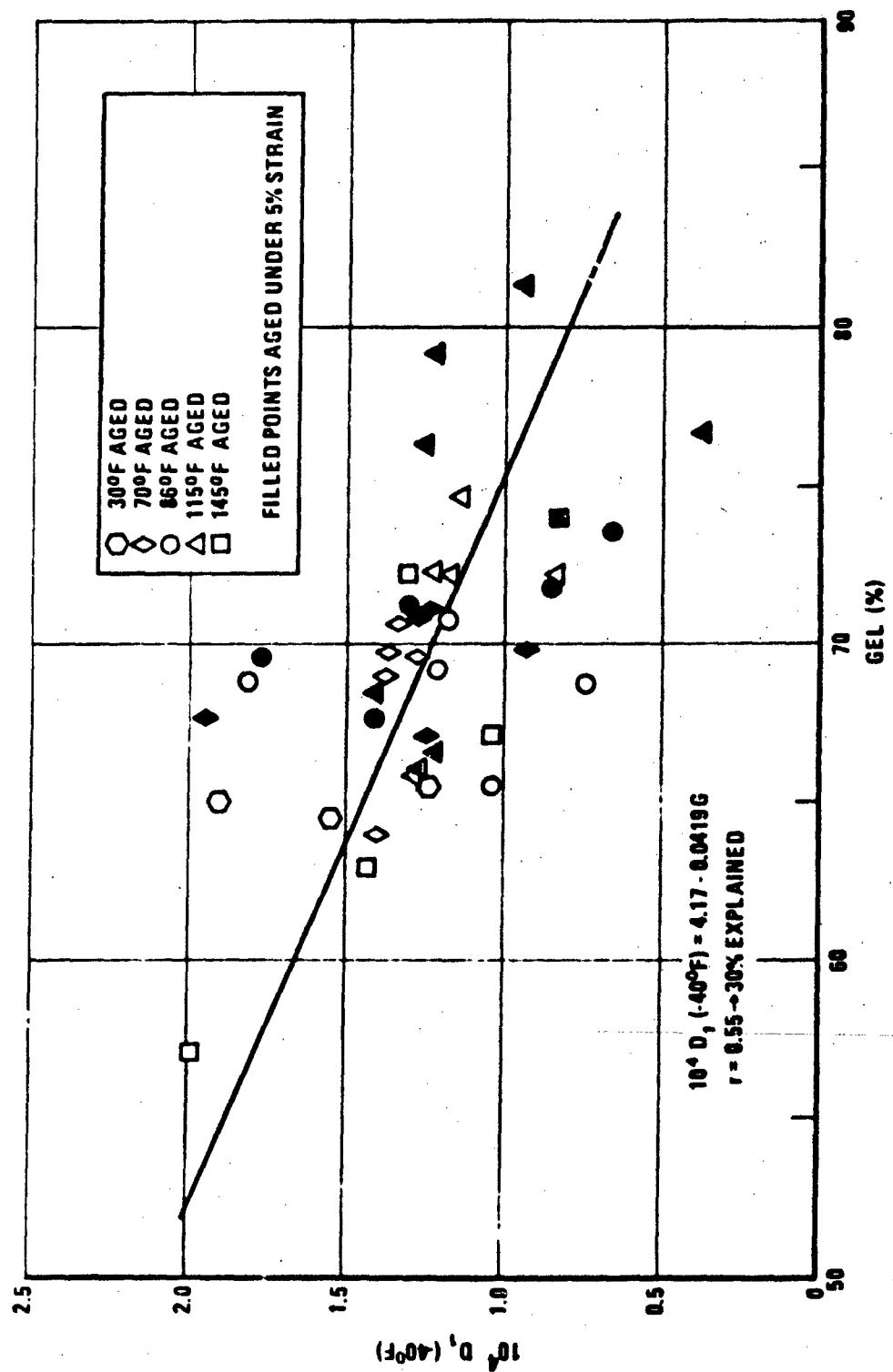
Figure 3-4 Compliance (-40°F) Versus Gel

$10^4 D_1 (-40°F) = 4.17 - 0.0419G$

$r = 0.55 \rightarrow 30\%$ EXPLAINED
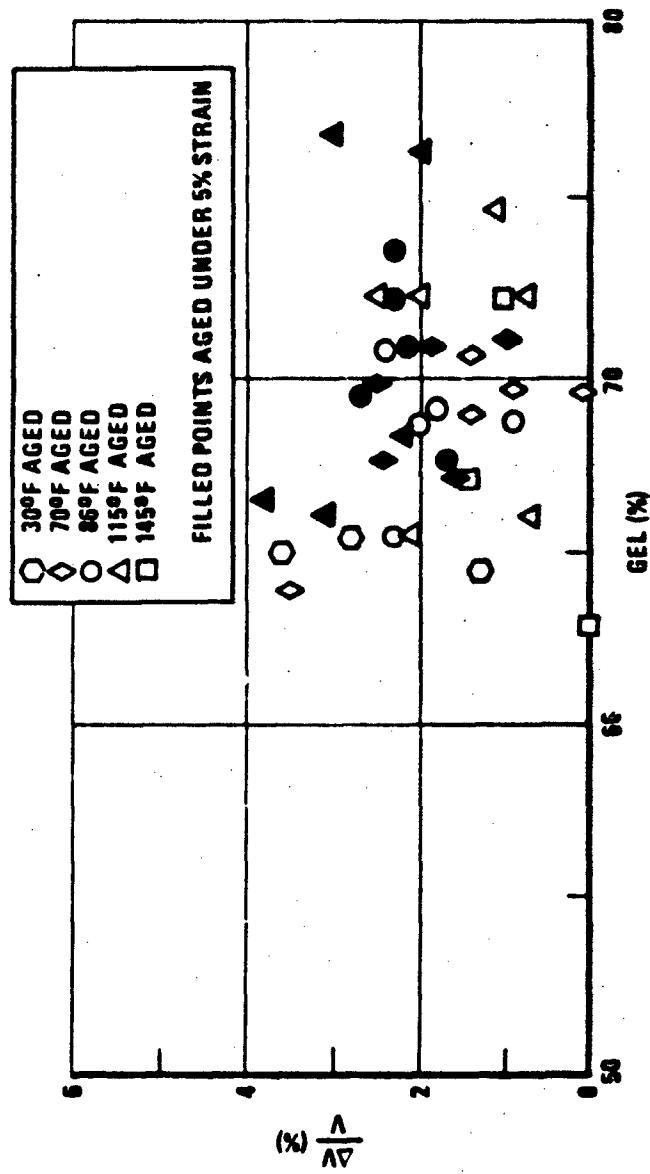
Figure 3-5 Dilatation Versus Gel
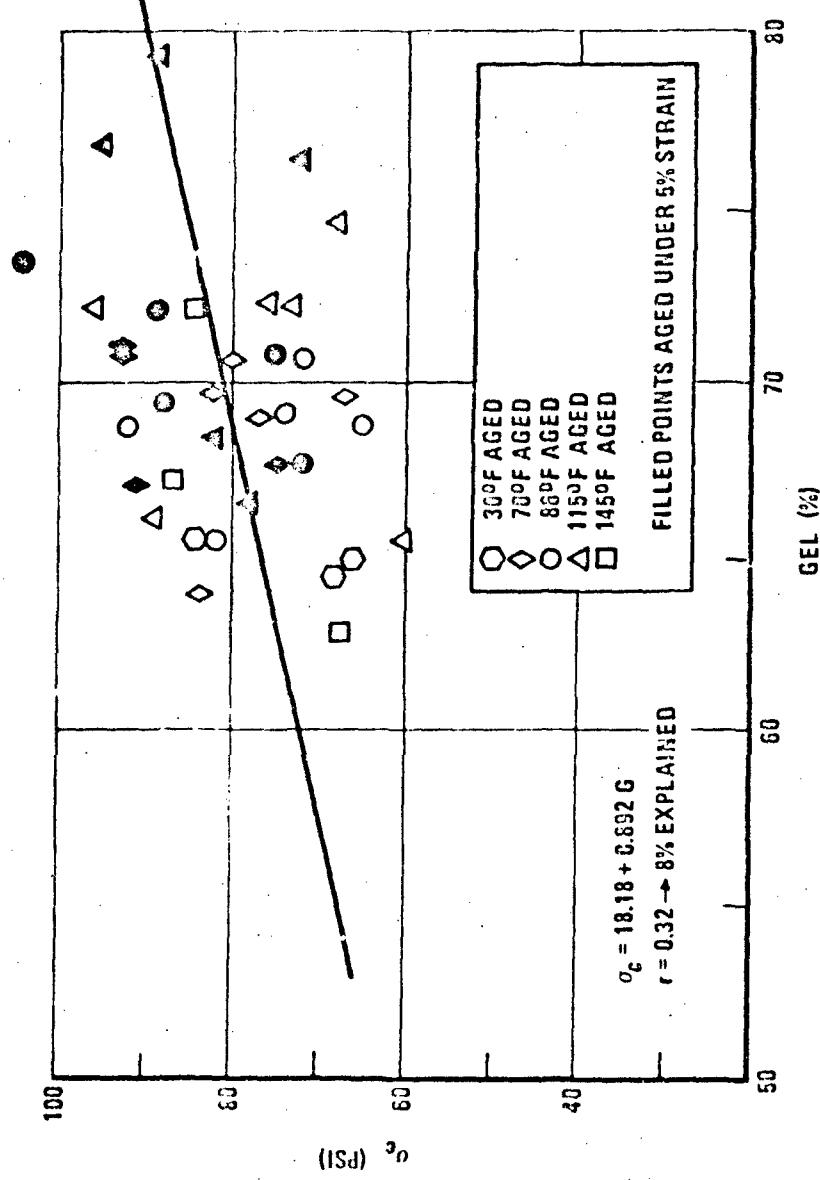
Figure 3-6   Critical Stress Versus Gel

data scatter inherent in such a program, the need for aging time corrections to be described below, and the fact that the program objective was primarily to demonstrate in principle that accelerated surveillance data could be employed for 70^0F aging rate predictions.

It was necessary to apply equations (3-1) and (3-2) iteratively to the data to arrive at final values for k, k_1, and k_2. This was required in order to circumvent certain problems:

(1) Delay in initiation of surveillance, estimated as an effective 10-week period at 70^0F. This had two consequences, namely that no experimental values were available for P^0 and that all nominal aging times at temperatures other than 70^0F had to be increased by an amount corresponding to the 10 weeks at 70^0F.

(2) Use of the 30^0F propellant "bank" to initiate higher temperature aging at various points along the program, which also necessitated corrections to nominal aging times.

Details of the calculational procedure are given in Appendix B. Results of the analysis are given in Tables 3-4 and 3-5 for gel, swell, D_1 (100^0F), D_1 (-40^0F), $\Delta V/V$, and σ_c. For the other parameters (n, γ_c, σ_c, crack rate) no aging trends were observable. In addition to the parameters of the log time equations, these tables present statistical evaluations of the goodness of fit in terms of: (1) the standard deviations of regression for linear (column 6) and quadratic (column 11) regressions, (2) the percent of variation explained by the linear regressions (column 7), and (3) the confidence of a significant improvement in fit by using the quadratic rather than linear expression for those cases where that confidence was at least 70 percent (column 12).

In the majority of cases the standard deviation of regression for the quadratic fit is either worse than for the linear fit or is only marginally improved (column 11 versus 6). Where the quadratic expression does provide significant improvement, this is for the most part for long-term aging at 145^0F. In those same instances the linear fit is usually very poor, as shown by the low percent explained.

Neglecting the long-term 145^0F results, both gel content and compliance at 100^0F generally follow closely to a linear log time aging behavior. The other parameters show a poorer statistical fit to linear (or quadratic) behavior and, except for swell, this is consistent with their poorer reproducibility as shown by the precision values given in Table 3-3. It should be noted, too, that more aging data points are available over a wider time span for gel, swell, and D_1 (100^0F) and the correlations for these properties should therefore have greater validity than those for D_1 (-40^0F), $\Delta V/V$, and σ_c. Careful examination of the data points along with the statistical correlations also demonstrates that as a general rule one is subjectively comfortable with a particular data fit if the percent explained exceeds 85 percent. The results in Tables 3-4 and 3-5 indicate that this subjective criterion is easily met by gel and D_1 (100^0F) and marginally met by dilatation. Subsequent discussion and quantitative conclusions, therefore, will emphasize gel and D_1 (100^0F).

Table 3-4

AGING RATES FOR GEL, D_1 (100°F), AND SWELL

Property	Temperature (°F)	Strain %	Linear Regression[1]				Quadratic Regression[2]				
			P⁰	k	s[3]	% [4] Explained	P⁰	k₁	k₂	s[3]	Confidence of Improvement[5]
Gel	30	0	52.7	5.95	1.22	94	52.6	7.24	-0.642	1.18	
	70	0	52.8	8.17	1.61	92	52.6	9.21	-0.380	1.73	
	86	0	53.0	9.05	0.85	98	52.7	10.8	-0.872	0.87	
	115	0	53.7	10.4	2.22	89	52.5	13.9	-1.61	2.24	
	145	0	53.3	13.9	1.29	96	52.6	14.7	-4.99	1.10	
	(to 13.6 weeks)										
	145 (to 95 weeks)	0	57.5	6.56	4.98	40	51.6	24.8	-8.77	2.93	80%
	70	5	53.2	8.69	1.80	91	52.3	11.6	-1.15	1.82	
	86	5	53.1	10.5	1.51	97	52.5	13.3	-1.49	1.32	
	115	5	52.0	14.0	2.44	93	53.1	11.1	-1.57	2.52	
	145	5	53.5	16.9	2.58	90	52.4	24.8	-6.79	2.81	
	(to 12.8 weeks)										
	145 (to 123 weeks)	5	59.0	6.69	6.16	29	52.1	28.3	-10.1	2.17	95%
Compliance $10^1 D_1$ (100°F)	30	0	2.61	-0.482	0.042	99	2.60	-0.513	-0.824	0.0025	>99%
	70	0	2.58	-0.676	0.087	96	2.61	-0.755	+0.0564	0.093	
	86	0	2.59	-0.753	0.106	96	2.59	-0.742	-0.106	0.119	
	115	0	2.46	-0.704	0.181	87	2.58	-1.06	+0.167	0.176	
	145	0	2.54	-1.08	0.123	94	--	--			
	(to 13.3 weeks)										
	145 (to 94 weeks)	0	2.16	-0.330	0.335	25	2.60	-1.74	+0.677	0.098	>99%
	70	5	2.57	-0.745	0.225	83	2.57	-0.733	+0.00433	0.243	
	86	5	2.58	-0.869	0.138	95	2.60	-0.960	+0.0411	0.153	
	115	5	2.33	-0.873	0.212	87	2.60	-1.66	+0.571	0.140	75%
	145	5	2.47	-1.45	0.218	90	2.64	-2.71	+1.11	0.148	75%
	(to 12.4 weeks)										
Swell	30	0	17.0	-1.16	0.81	58	17.0	-2.65	+0.744	0.97	
	70	0	16.8	-2.40	1.20	63	16.7	-2.13	-0.125	1.29	
	86	0	16.2	-2.40	1.11	68	16.8	-5.34	+1.51	1.05	
	115	0	15.8	-3.01	0.95	79	16.6	-5.38	+1.11	0.86	
	145	0	15.8	-3.58	1.27	74	16.7	-7.13	+1.97	1.09	
	(to 64 weeks)										
	145 (to 95 weeks)	0	14.0	-0.496	2.77	2	17.2	-10.31	+4.57	2.01	70%
	70	5	16.3	-2.58	1.13	69	16.8	-4.07	+0.685	1.17	
	86	5	16.1	-2.69	1.78	48	16.7	-5.43	+1.42	1.89	
	115	5	16.0	-3.24	1.09	77	16.4	-4.34	+0.521	1.13	
	145	5	16.1	-5.20	1.36	74	16.8	-10.39	+4.60	1.57	
	(to 12.5 weeks)										
	145 (to 123 weeks)	5	14.4	-1.89	2.17	16	16.7	-9.14	+3.59	1.14	85%

[1] $P = P^0 + k \log t$

[2] $P = P^0 + k_1 \log t + k_2 (\log t)^2$

[3] s = standard deviation of regression

[4] $\left[1 - \frac{n-1}{n-2}(1-r^2)\right] \times 100$, where n = # data points and r = regression correlation coefficient

[5] Standard F test, where F = reduction in mean square deviation due to quadratic term/mean square deviation of quadratic regression.

Table 3-5

AGING RATES FOR D_1 (-40°F), CRITICAL STRESS, AND DILATATION

Property	Temperature (°F)	Strain %	Linear Regression[1]				Quadratic Regression[2]				Confidence of Improvement[5]
			P^0	k	s[3]	% Explained[4]	P^0	k_1	k_2	s[3]	
Compliance $10^4 D_1$(-40°)	30	0	2.59	-0.521	0.18	74	2.57	-1.60	0.507	0.21	
	70	0	2.59	-0.616	0.15	90	2.58	-0.523	-0.046	0.16	
	86	0	2.63	-0.787	0.38	64	2.57	-0.331	-0.245	0.41	
	115	0	2.53	-0.797	0.20	87	2.61	-1.07	0.135	0.20	
	145	0	2.62	-1.10	--	60	--	--	--	--	
(to 14.5 weeks) 145		0	2.30	-0.452	0.49	23	2.60	-1.71	0.614	0.44	80%
(to 96 weeks) 70		5	2.66	-0.675	0.32	69	2.57	0.0348	-0.353	0.32	
	86	5	2.67	-0.831	0.38	67	2.58	-0.213	-0.330	0.40	
	115	5	2.54	-0.867	0.34	72	2.63	-1.18	0.152	0.37	70%
	145	5	2.66	-1.40	0.53	63	--	--	--	--	
(to 11.9 weeks)											
Dilatation ΔV/V	30	0	6.8	-2.22	0.93	83	6.7	0.466	-3.53	0.67	
	70	0	7.0	-2.60	1.11	75	6.7	1.23	-1.93	1.05	
	86	0	6.7	-2.47	0.79	82	6.7	-3.01	0.280	0.88	
	115	0	6.6	-2.70	0.99	76	6.7	-3.77	0.537	1.06	
	145	0	6.9	-3.19	0.77	92	6.7	-1.25	-1.01	0.74	
(to 109 weeks) 70		5	6.8	-2.45	0.70	87	6.7	-0.497	-0.960	0.71	
	86	5	6.7	-2.31	0.56	89	6.7	-2.74	0.224	0.62	
	115	5	6.6	-2.12	0.74	78	6.7	-3.47	0.734	0.78	
Critical Stress, σ_c	30	0	53.7	9.86	9.5	41	54.0	-8.90	9.59	13.1	
	70	0	53.1	12.3	6.7	62	54.0	3.10	4.53	7.2	
	86	0	53.4	12.5	9.7	38	53.9	6.59	3.13	10.8	
	115	0	53.1	13.2	12.1	26	53.3	12.2	0.494	13.3	
	145	0	53.1	17.2	--	67	--	--	--	--	
(to 71 weeks) 145		0	56.5	11.5	11.8	26	53.3	32.2	-10.7	12.8	
(to 102 weeks) 70		5	50.1	18.0	7.8	73	53.9	-22.5	20.1	3.6	
	86	5	51.2	18.0	12.2	47	53.6	-7.23	13.3	12.7	>99%
	115	5	51.3	17.9	8.1	65	53.8	-1.10	11.3	7.9	

(1) - (5) See footnotes of Table 3-4.

Figures 3-7 through 3-12 present aging curves for gel, D_1 (100^0F), and swell which were calculated using parameters from Tables 3-4 and 3-5. The linear regression parameters were used except where the quadratic behavior provided a significantly better description of the aging pattern. Where the long-term 145^0F pattern appears to be better described by a quadratic, the short-term linear regression line is also presented for comparison. To avoid undue confusion, data points are included only for 70 and 145^0F aging.

From the results of this analysis it is evident that when sufficient data are available the aging behavior of this ANB-3066 batch, at temperatures $\leq 115^0F$ and for aging times up to 130 weeks, can be quantitatively described by equations which are linear in logarithmic time. At the higher temperatures there is some evidence that the initial "hardening" process, which is linear in log time, is being overtaken (e.g., after 10 to 15 weeks at 145^0F) by a reversion ("softening") process, such that an overall quadratic rate equation with constants of opposite sign becomes more suitable. Unfortunately, the 145^0F data are not extensive enough to define the course of this reversion process very accurately, nor are the lower temperature data sufficiently long term to establish with confidence whether or when a reversion process may become important under conditions approaching silo storage. Although quadratic terms have been calculated for the lower aging temperatures, these cannot be identified with a reversion process with a great deal of assurance.

3.2.3 Temperature and Strain Dependence of Aging Rates

To make use of accelerated surveillance data to predict low temperature storage life it must be possible to perform a temperature extrapolation of aging rates. This possibility was examined for the various aging rate constants (k, k_1, k_2) using a conventional Arrhenius approach, i.e.,

$$k = k_0 \exp\left[\frac{-B}{RT}\right] \qquad (3-3)$$

Figures 3-13 and 3-14 demonstrate for gel and D_1 (100^0F) that the Arrhenius equation is indeed followed by the rate constants calculated using either the linear or quadratic aging rate equations. Reflecting the uncertainty in the quadratic behavior, it should be noted that not all the k values could be used in this correlation, e.g., the 30^0F point in Figure 3-14 and two values of opposite sign for D_1 (100^0F) were not used.

Regression analyses were performed to obtain the parameters of equation (3-3) for those cases where statistically significant rate constants were available. The k_0 and B (apparent activation energy) values are summarized in Table 3-6. The apparent activation energies for the hardening process (k) are all quite small indicating that the process is diffusion controlled and/or is free radical. From a similar linear analysis of shorter term aging data for another batch of ANB-3066 Thiokol reports a B value for tensile properties of about five (Ref. 6). Why their value should be so much greater than that found here is not clear, although a rather crude analysis
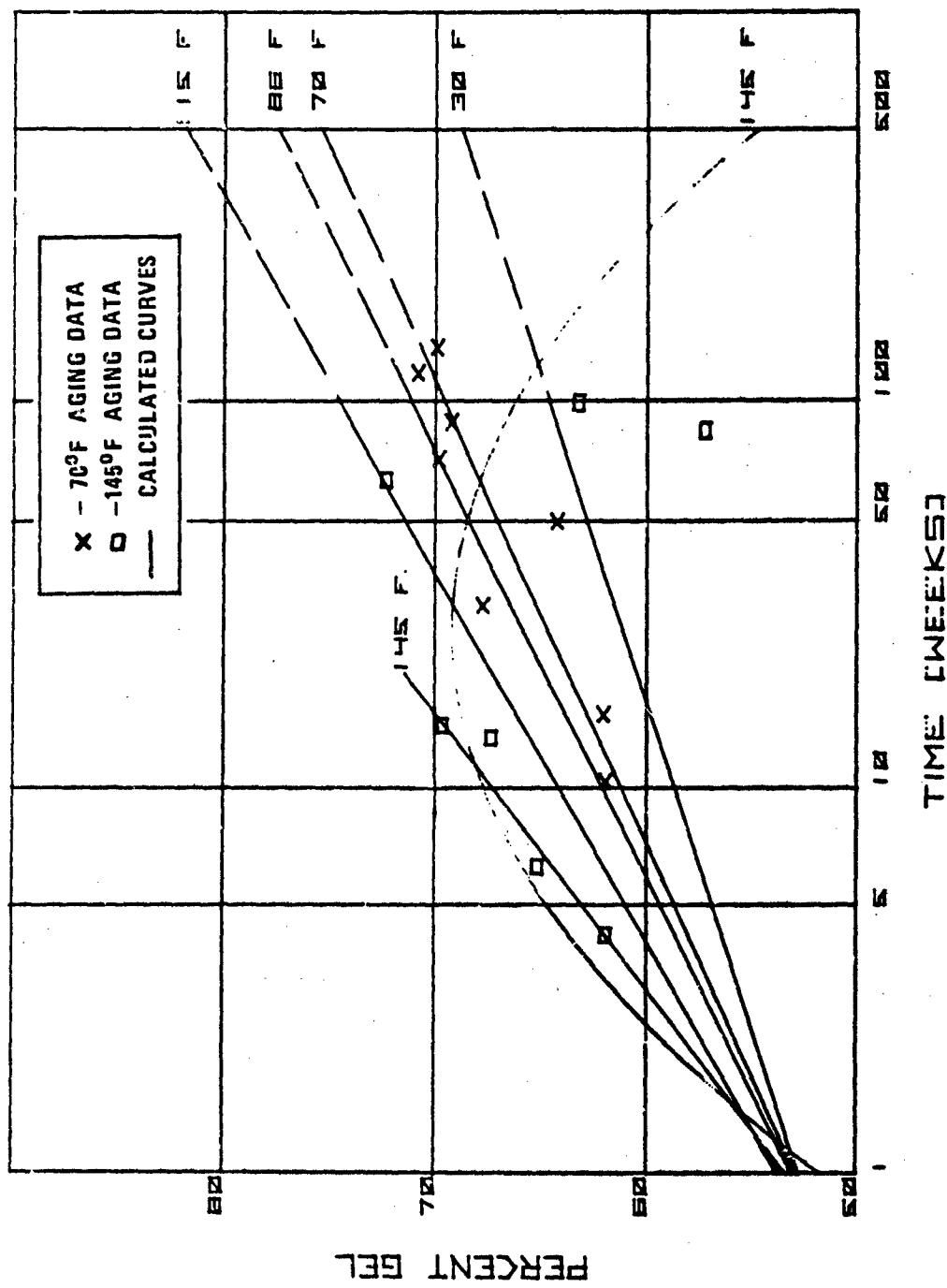
Figure 3-7 Effect of Aging at 0% Strain on Gel Content
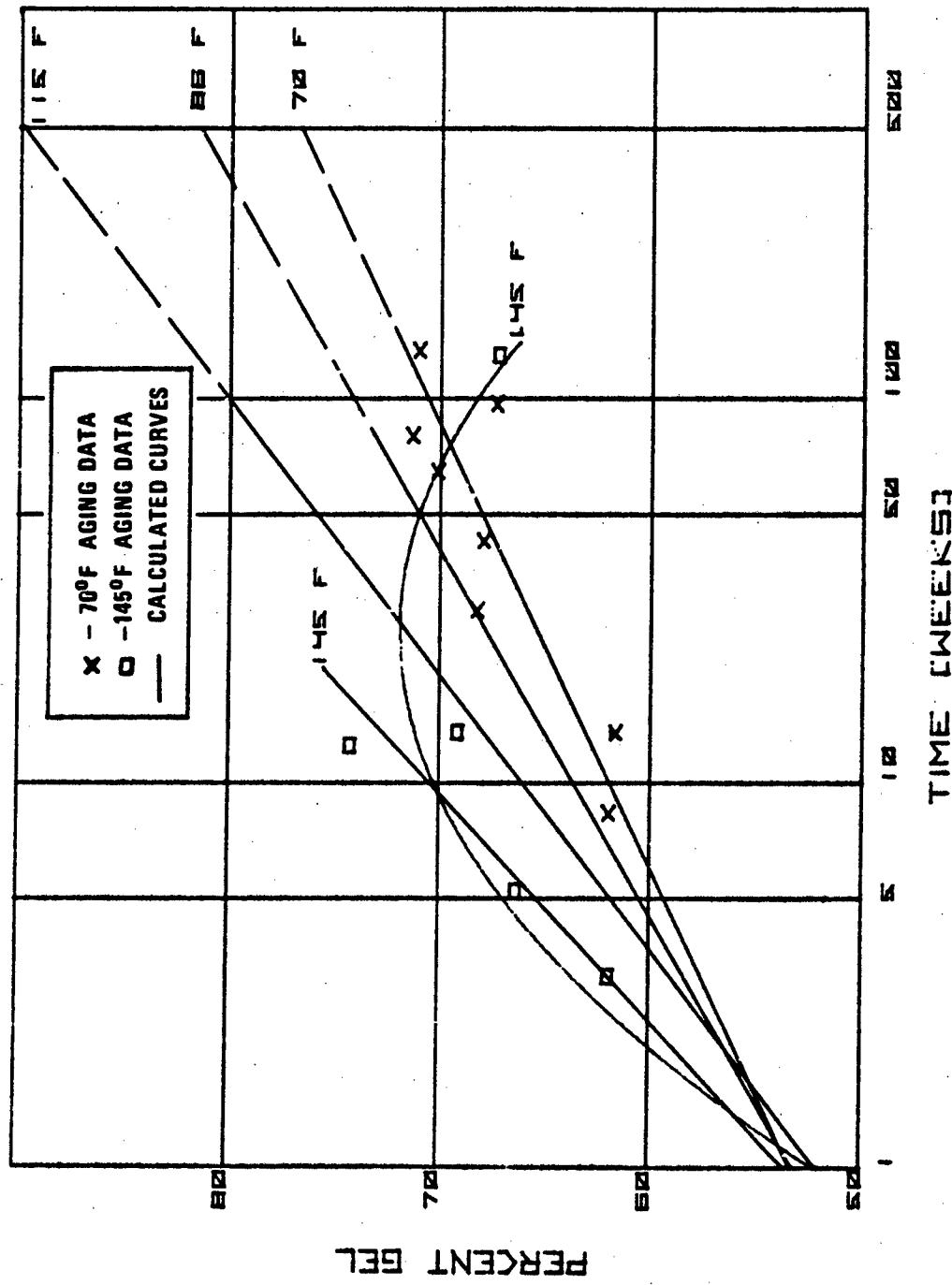
Figure 3-8 Effect of Aging at 5% Strain or Gel Content
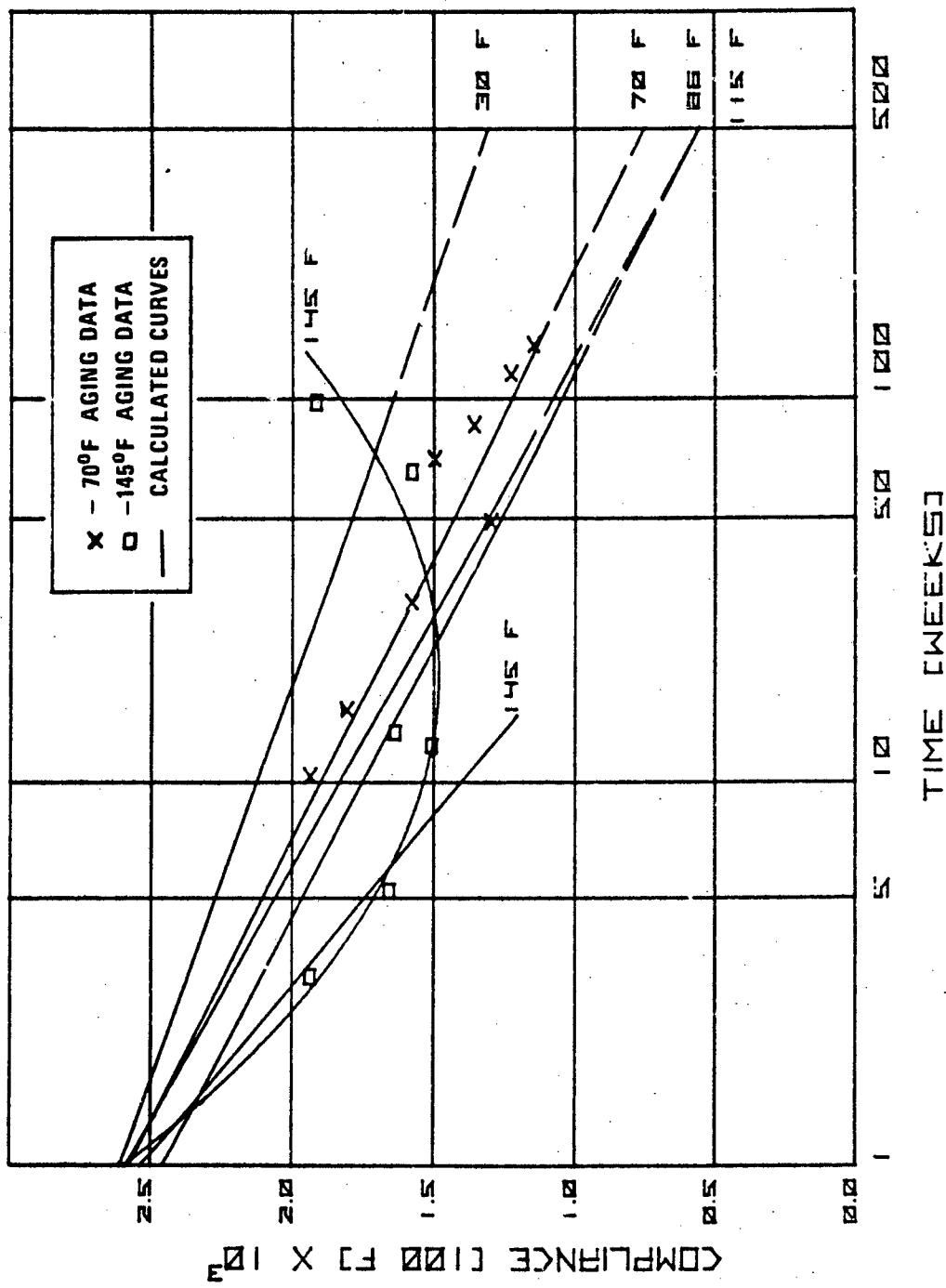
Figure 3-9   Effect of Aging at 0% Strain on Compliance, D_1 (100°F)
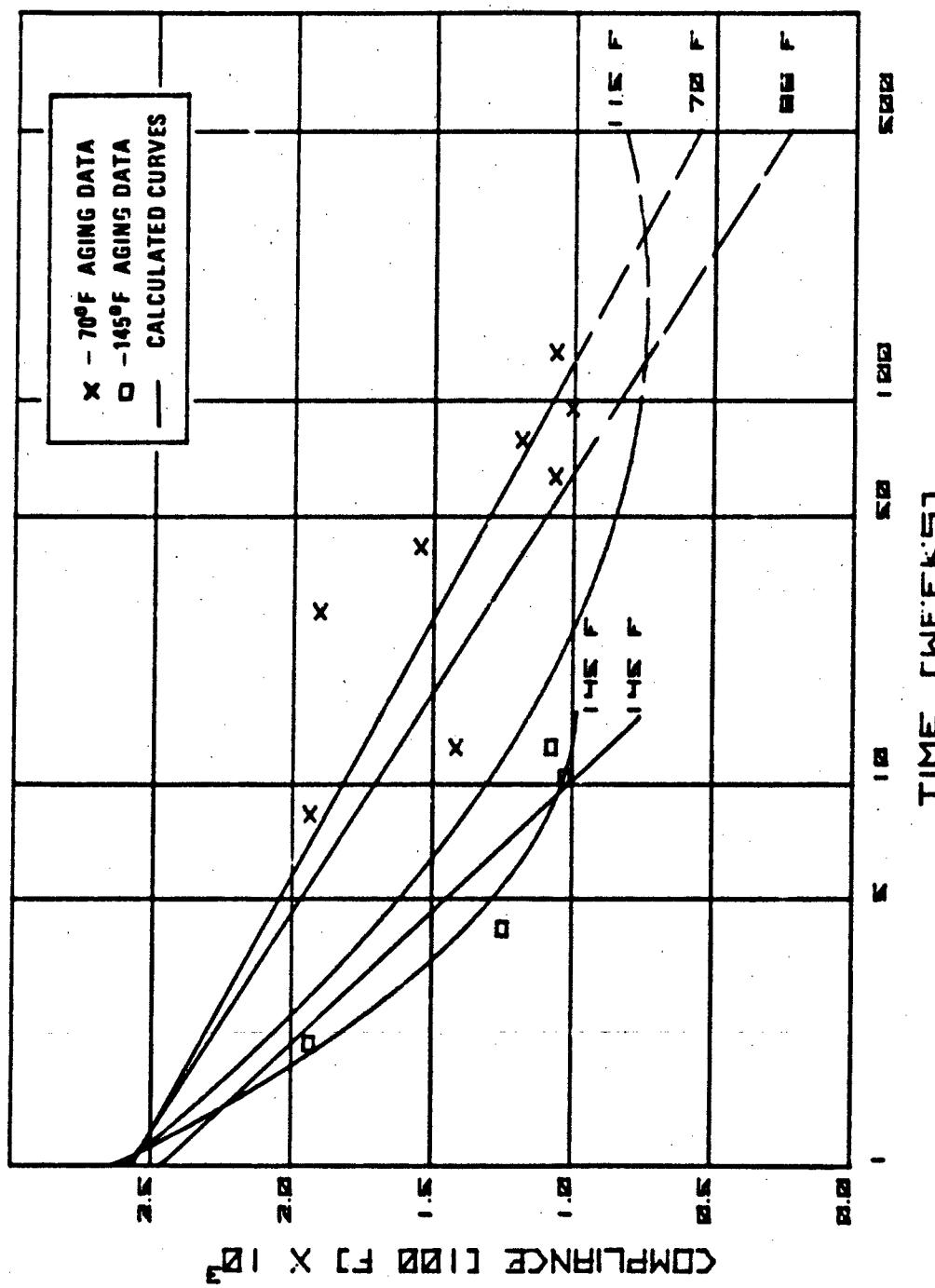
Figure 3-10   Effect of Aging at 5% Strain on Compliance, D_1 (100°F)
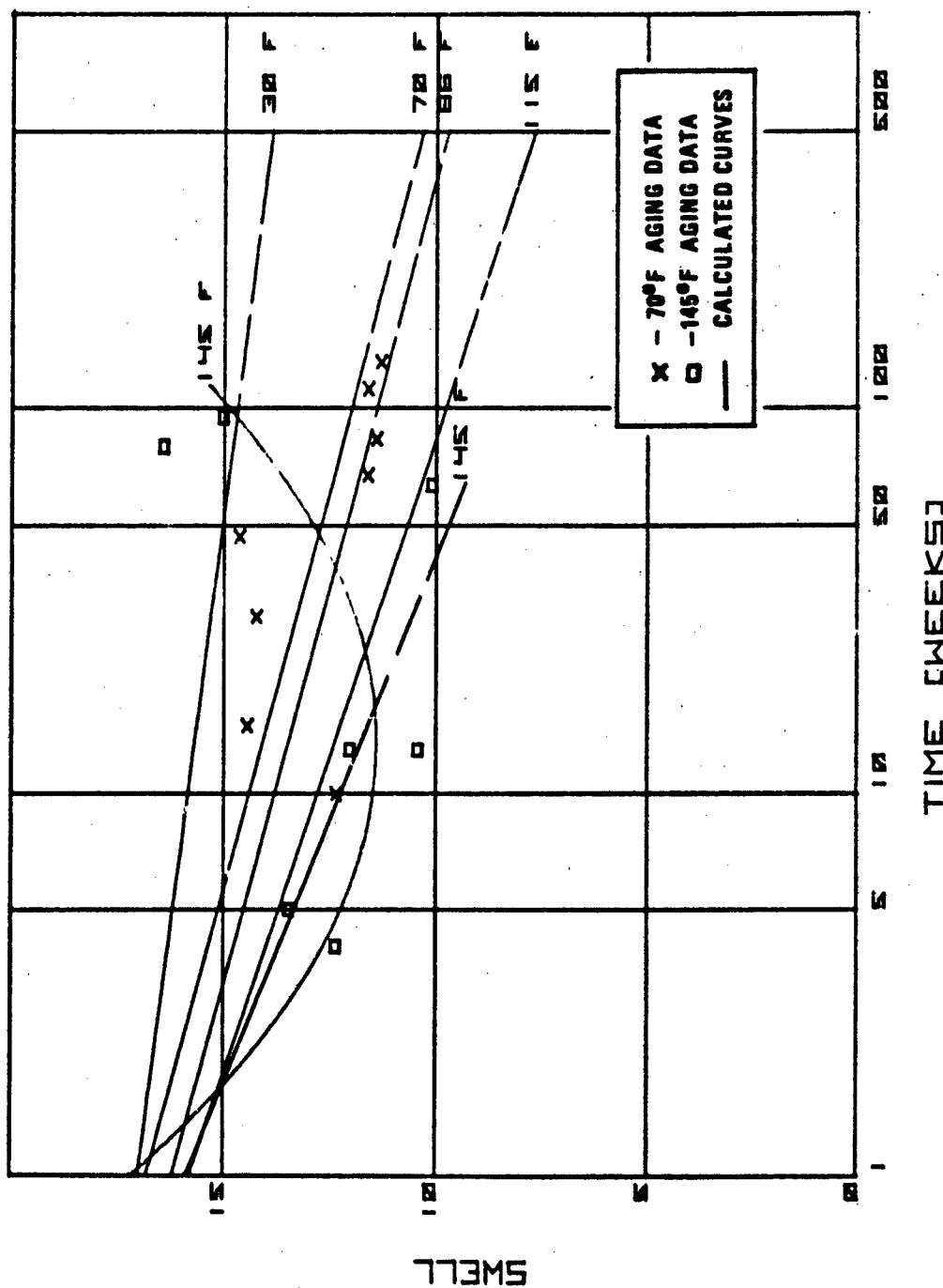
Figure 3-11   Effect of Aging at 0% Strain on Degree of Swell
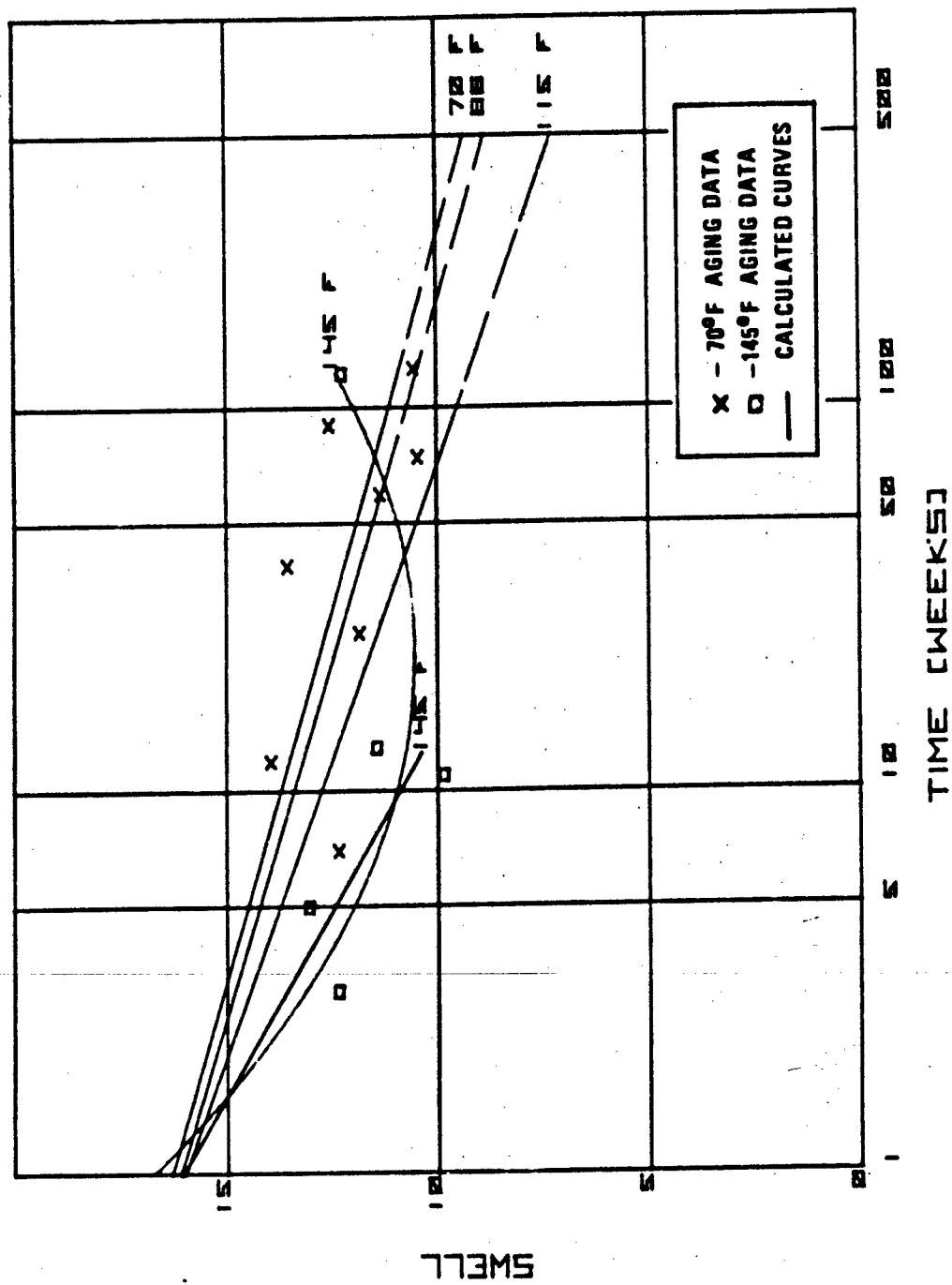
Figure 3-12 Effect of Aging at 5% Strain on Degree of Swell
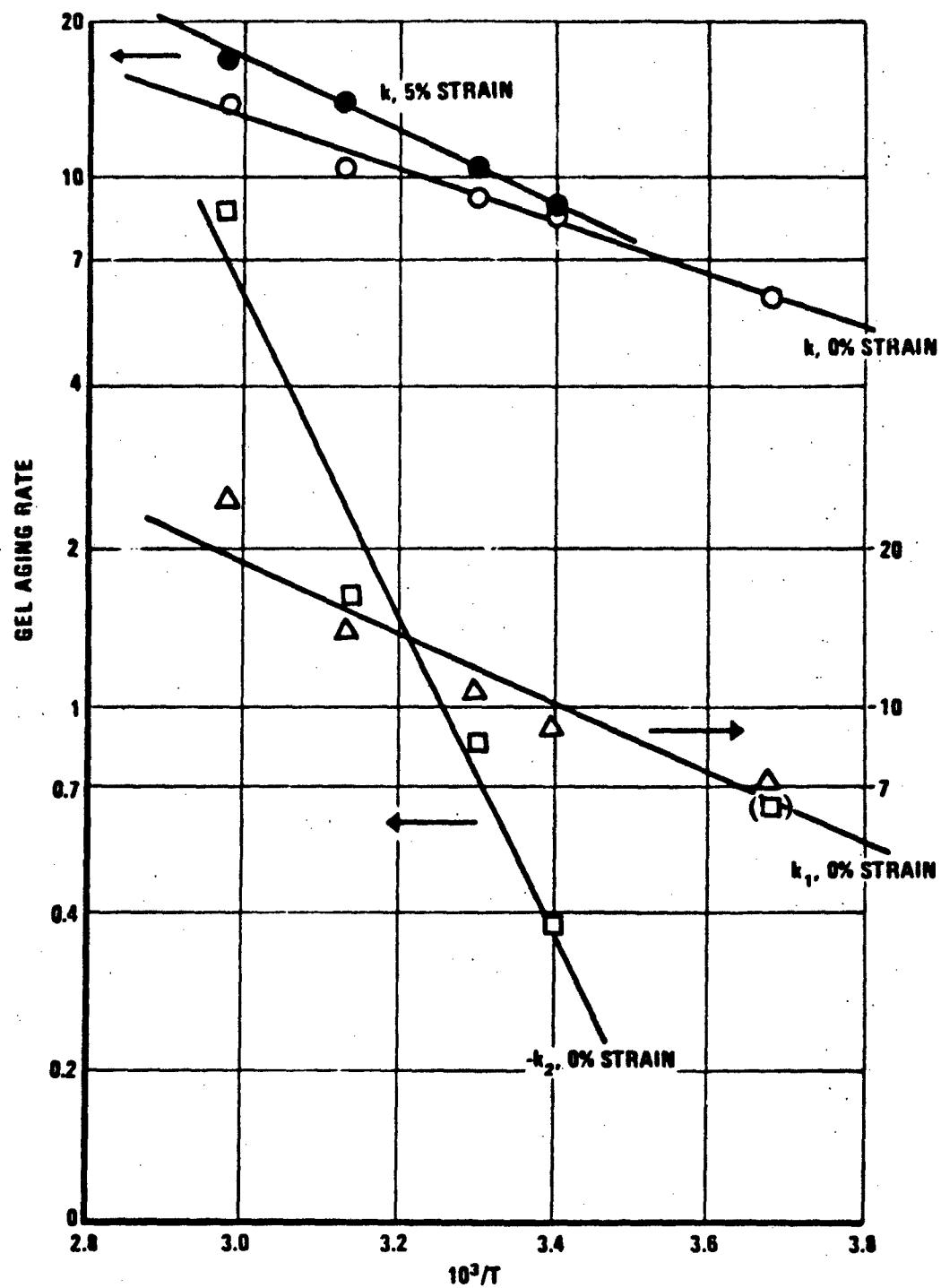
Figure 3-13   Temperature Dependence of Gel Aging Rates
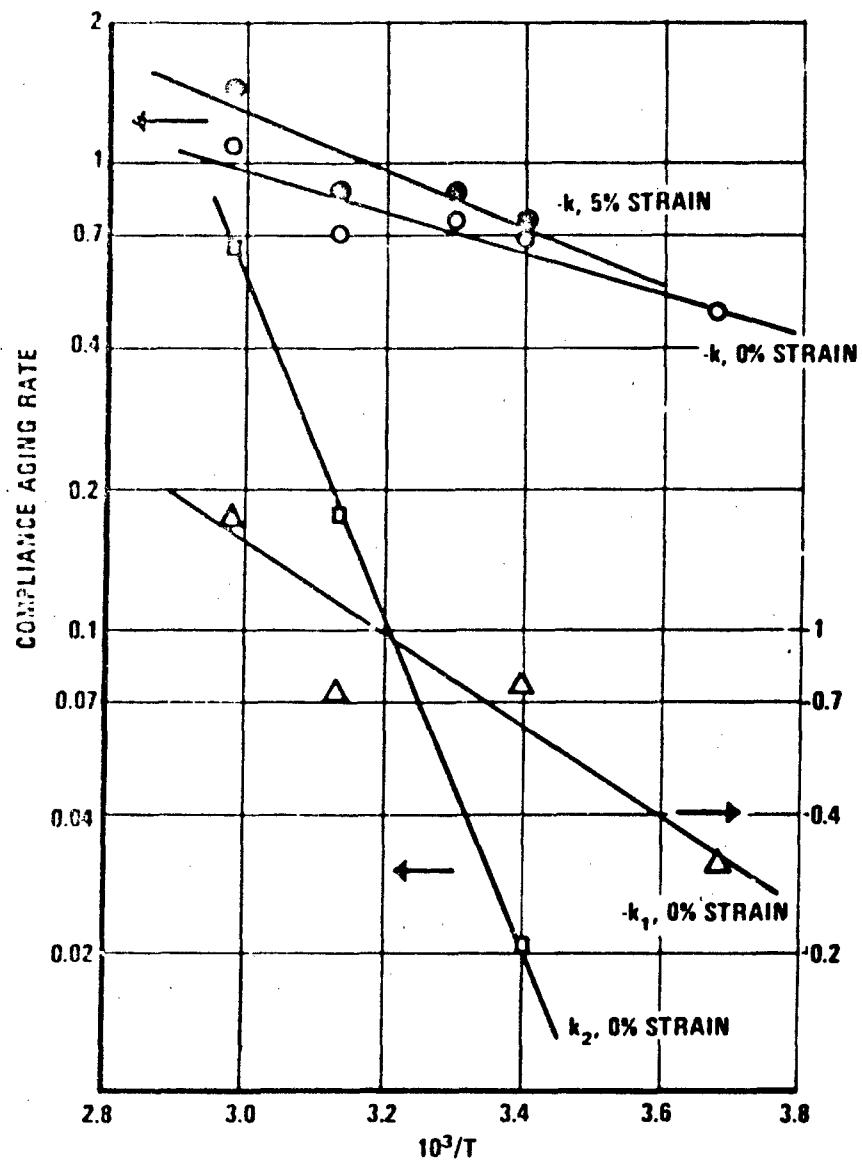
Figure 3-14 Temperature Dependence of Compliance (100°F) Aging Rates

Table 3-6

ARRHENIUS PARAMETERS[1]

Property	k			k_1			k_2		
	$\log k_0$	B	% Explained[2]	$\log k_{10}$	B	% Explained[2]	$\log k_{20}$	B	% Explained[2]
Gel, 0% Strain	2.605	2.29	97	3.280	3.09	90	9.891	14.0	93
5% Strain	3.295	3.18	99	4.042	4.05	99	7.573	10.2	92
D_1(100°F), 0%	1.283	2.00	81	3.205	4.62	96	8.572	13.6	96
5%	1.925	2.80	70	4.488	6.28	>99	16.505	25.2	93
Swell, 0%	2.594	3.11	91						
5%	2.783	3.26	83						

[1] $\log k = \log k_0 - \dfrac{B}{2.3R} \left(\dfrac{1}{T}\right)$

[2] See footnote (4) of Table 3-4.

of older Aerojet data on ANB-3066 (Ref. 7) indicates a distinct batch-to-batch variation in B (see Figure 3-15) which apparently is not related to the unaged modulus level. Interestingly, the B value for the postulated reversion process is several fold greater than that for the hardening process.

For the most part the effect of aging under strain is to increase the apparent activation energy of the hardening process and to increase the aging rate significantly at $145^\circ F$ but only slightly at $70^\circ F$. This is illustrated by the 0 and 5-percent strain Arrhenius plots for k in Figure 3-13 and 3-14 and by the relative aging rates (k/P^0) listed in Table 3-7. (Whether the opposite effects for dilatation are real is not now certain.)

Thus it appears that a conventional Arrhenius treatment provides a means of extrapolating ANB-3066 aging rates at high temperatures to aging rates which are applicable under silo storage conditions. Although aging under 5-percent strain has only small effect upon the aging rate at $70^\circ F$, it will be seen later (Subsection 3.2.5) that this can have a major effect upon predicted service life because of the relatively long times involved and the logarithmic time dependence. However, the combination of moderate temperature and strain aging could offer a means of further accelerating aging without having to resort to undesirably high temperatures; for example, aging at $145^\circ F$ under 5 percent strain is equivalent to aging unstrained at approximately $195^\circ F$ with regard to rate of increase in gel content.

3.2.4 Comparison With Other ANB-3066 Aging Data

Aging data are available for a number of other ANB-3066 batches with which the aging patterns observed in this program can be compared. Figure 3-16, for example, compares the LPC regression curves for compliance changes at 145 and $70^\circ F$ with data reported by Aerojet (Ref. 7) for tensile modulus changes of three different batches at 150 and $80^\circ F$. For each Aerojet batch, the $1/E$ values were normalized for convenience to approximately match the magnitude of LPC's compliance values. The batch-to-batch variations in the aging rates of $1/E$ are obviously large. At 70 to $80^\circ F$ the LPC aging rate is intermediate among the Aerojet, but at 145 to $150^\circ F$ the initial aging rates of all three Aerojet batches are much above that of the LPC batch. Furthermore, the $150^\circ F$ data do not follow a simple linear logarithmic time aging trend although more extended aging would be required to establish whether a reversion is occurring or whether the modulus is approaching a steady state.

Figure 3-17 presents a similar comparison between compliance measured on the batch at LPC and relaxation modulus measured on the batch studied by Thiokol (Ref. 6). Again, the $1/E_r$ values were normalized to overlap LPC's compliance values. At 70 to $75^\circ F$, the two aging rates are quite close. However, at increasing temperatures the Thiokol aging rate becomes progressively greater than LPC's, in line with the higher activation energy previously discussed. While the 80 and $115^\circ F$ aging points would be adequately described by a linear relationship, the $150^\circ F$ $1/E_r$ points clearly would be better described by a curvilinear function; the latter is, of course,
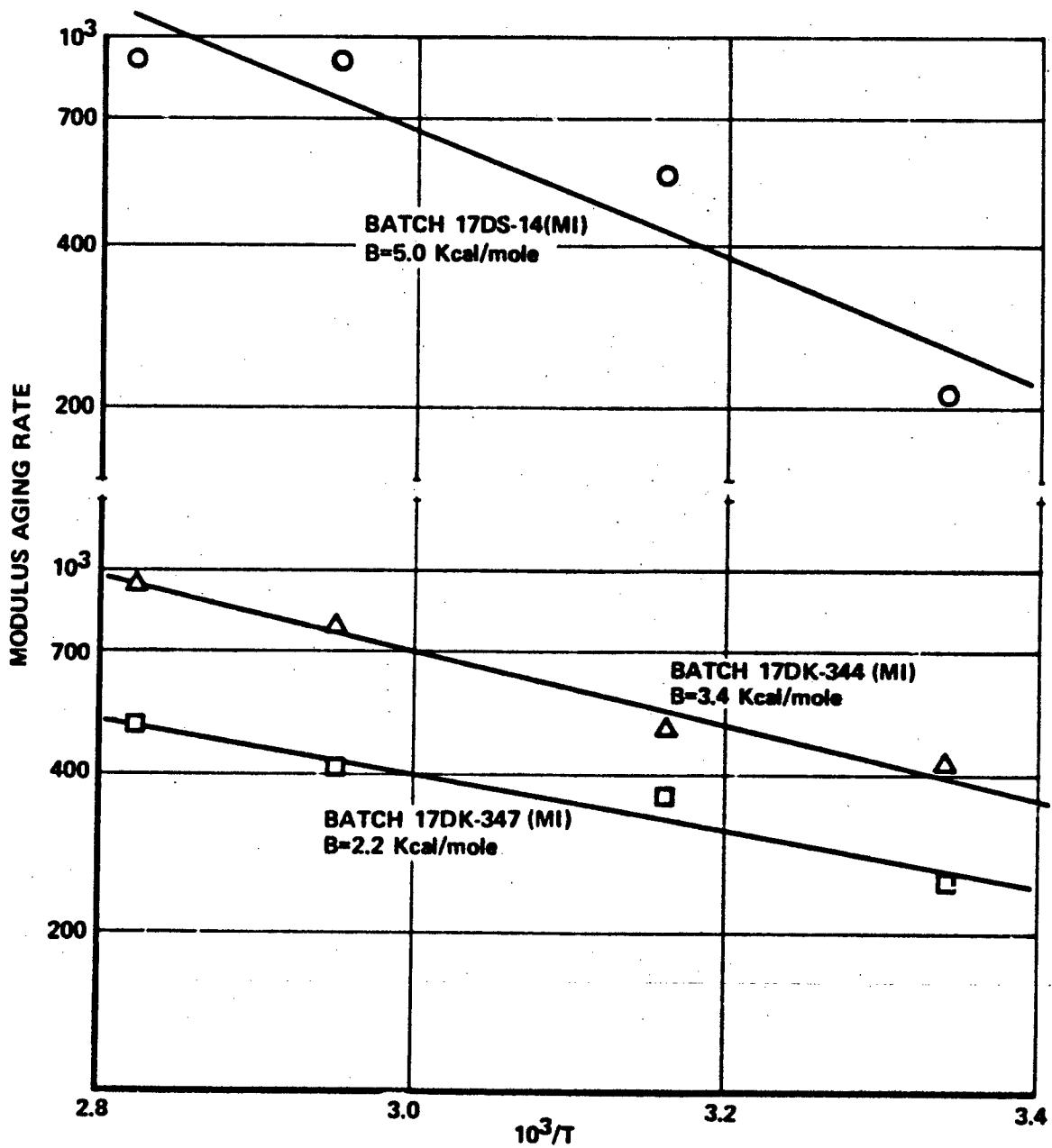
Figure 3-15   Batch Variations in Temperature Dependence
of Modulus Aging Rate (Aerojet data, Ref. 7)

Table 3-7

RELATIVE AGING RATES[1]

Property	Aging Strain	Relative Rate of Change[2]	
		70°F	145°F
Gel	0	0.16	0.26
	5	0.16 (0%)	0.32 (23%)
$D_1 (100\%)$	0	-0.26	-0.43
	5	-0.29 (12%)	-0.59 (30%)
Swell	0	-0.14	-0.23
	5	-0.16 (14%)	-0.32 (48%)
$\Delta V/V$	0	-0.38	-0.46
	5	-0.36 (-5%)	--

---

[1] k/P^0

[2] Numbers in parenthesis represent the percentage increase in rate between 0 and 5% strain.
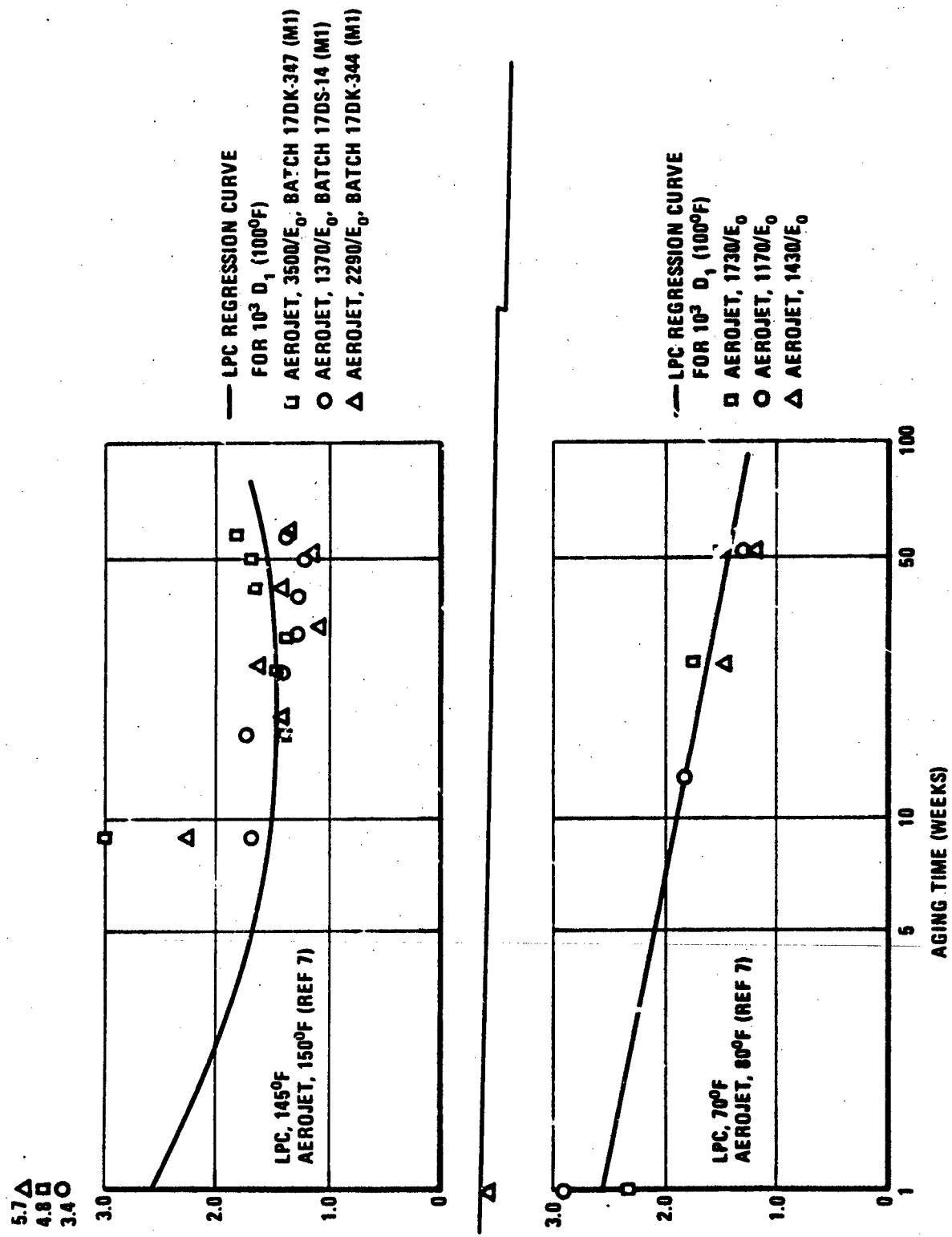
Figure 3-16 Comparison of LPC and Aerojet Aging Data For ANB-3066; Batch Variations
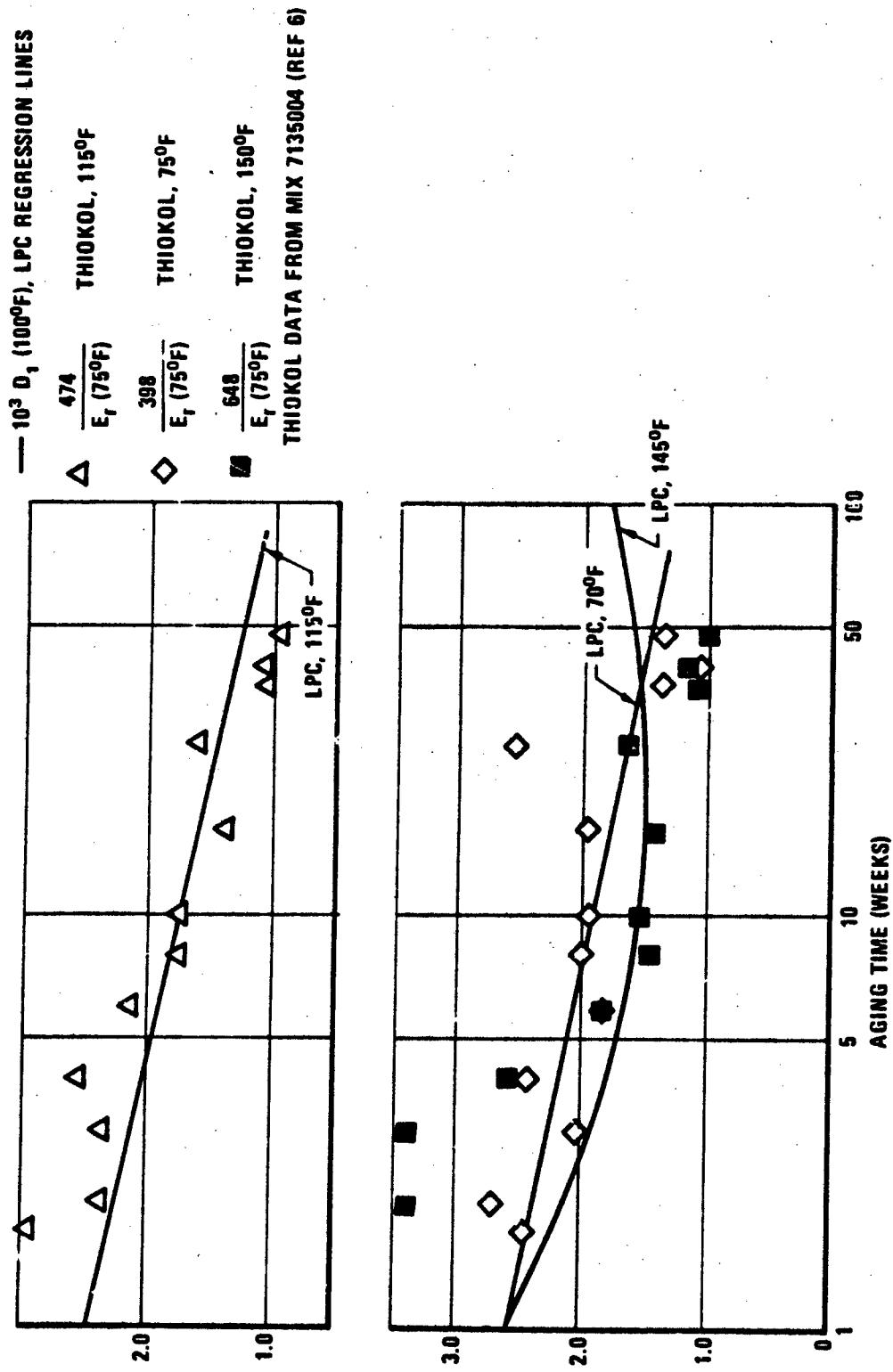
Figure 3-17   Comparison of LPC Compliance and Thiokol Stress Relaxation
Data For Aging of ANB-3066

qualitatively consistent with Thiokol's use of a linear log time function to describe the aging changes in E_r itself instead of $1/E_r$.

The LPC and Thiokol (Ref. 6) gel content results are compared in Figure 3-18, in this case without employing any normalization factor. In contrast to the compliance/modulus comparison, here the LPC data indicate a somewhat stronger rate of change than do the Thiokol results. Moreover, the Thiokol values at 115 and 150°F indicate an approach to a steady state although the question of a reversion would require longer term data to answer.

All of the above comparisons involved approximately 1-year aging data from Aerojet and Thiokol and 2-year aging data from LPC. Figures 3-19 and 3-20, on the other hand, are concerned with comparisons of long-term (7 to 8 years) 80°F aging data for ANB-3066 with the predictions from LPC's 70°F aging equations. Figure 3-19 compares LPC's 70°F compliance equation with Aerojet 1/E values for a different batch, the latter being normalized to overlap the LPC regression line. Although the LPC aging rate is slightly larger, the agreement certainly falls within the batch-to-batch variations noted above. The Aerojet batch may have reached a steady state, in which case the LPC linear regression line would increasingly deviate beyond the 7-year point.

Finally, in Figure 3-20 the same LPC 70°F regression line for compliance (100°F, 60 psi) is compared with Hill AFB compliance (77°F, 80 psi) values on 15 different batches of aged ANB-3066, without employing any normalizing factor to correct the Hill values. Obviously, if such a normalization had been performed the observed and predicted compliance values would be well within the batch-to-batch data scatter.

In summary of these comparisons the following points are noted:

- Rather large differences in aging behavior are exhibited by different batches, particularly at higher temperatures. As pointed out in Appendix C, batch variations are to be expected in view of the fact that propellants normally cured are only slightly beyond the very steep portion of the gel/extent of reaction curve. Therefore, only small variations in effective stoichiometry or in cure schedule can significantly change the initial gel content and thereby the apparent aging behavior.

- At low temperatures (~70°F) it is probable that aging behavior can be described by a linear log time relation up to 1 to 2 years, beyond that point a slightly curvilinear expression may be more suitable in reflecting attainment of a steady state or some degree of reversion.

- At higher temperatures, aging behavior for some parameters exhibits increasing degrees of nonlinearity as a function of log time. LPC data give indication of a reversion process occurring while other data seem more consistent with attainment of a steady state. Longer term data at various temperatures and with
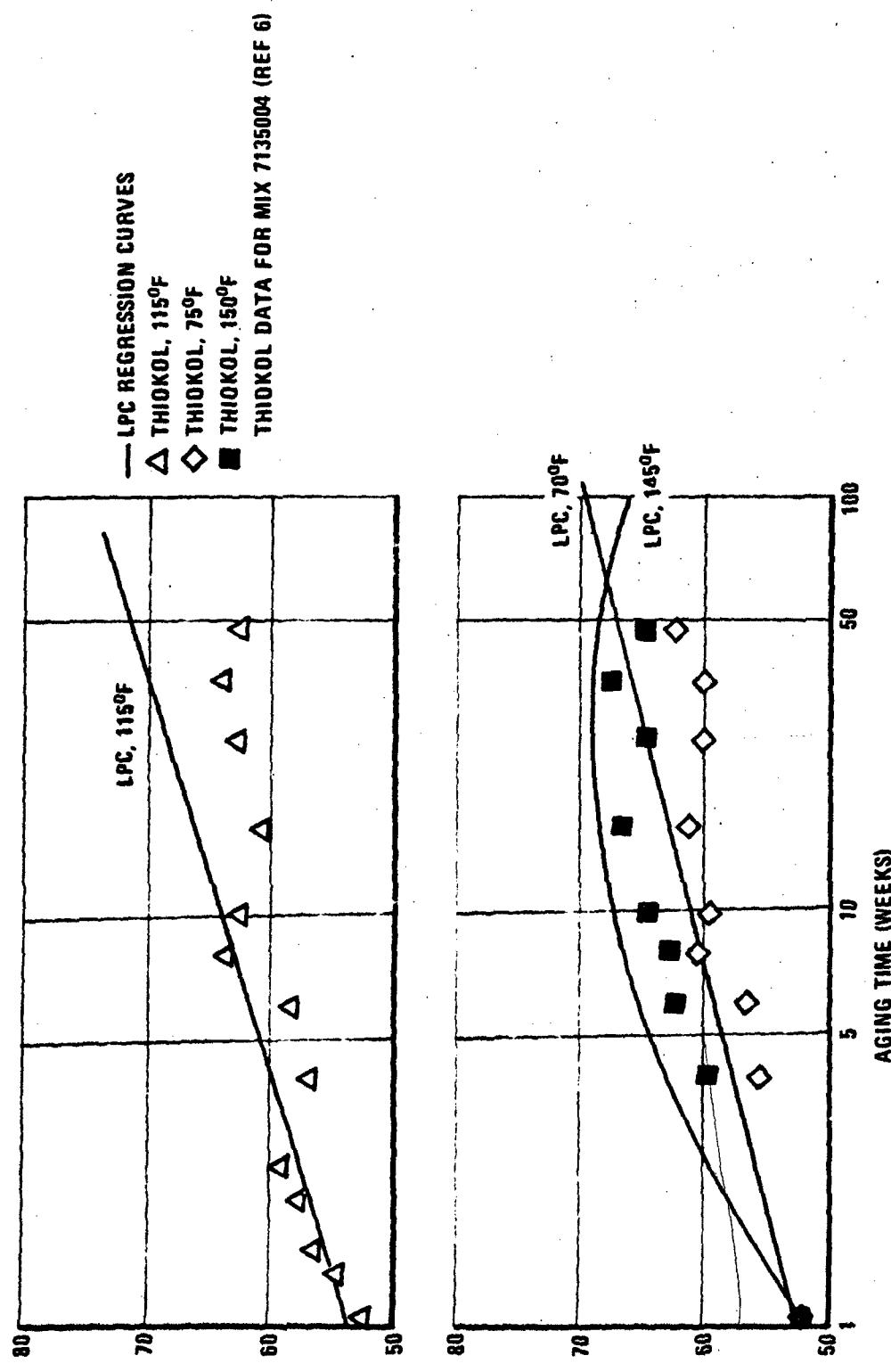
Figure 3-18 Comparison of LPC and Thiokol Gel Content Data For Aging of ANB-3066
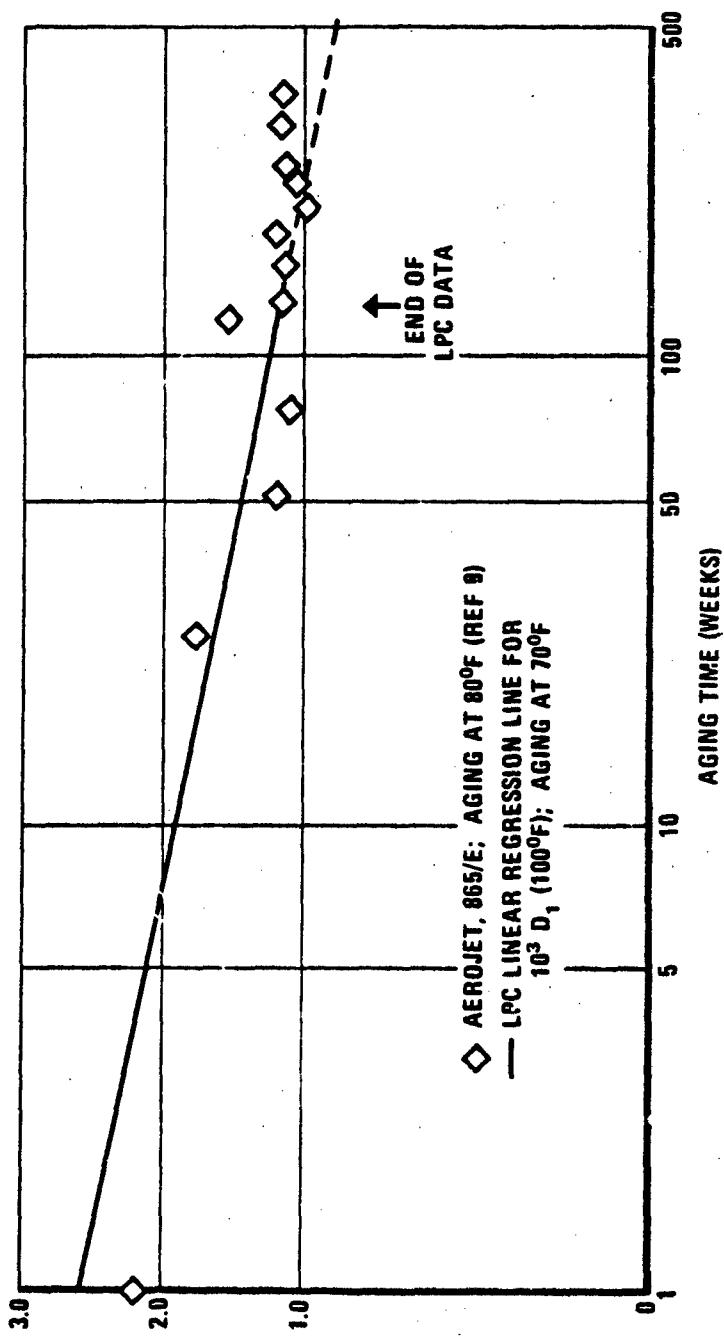
Figure 3-19 Long-Term Aging: Comparison of LPC Compliance and Aerojet Tensile Modulus
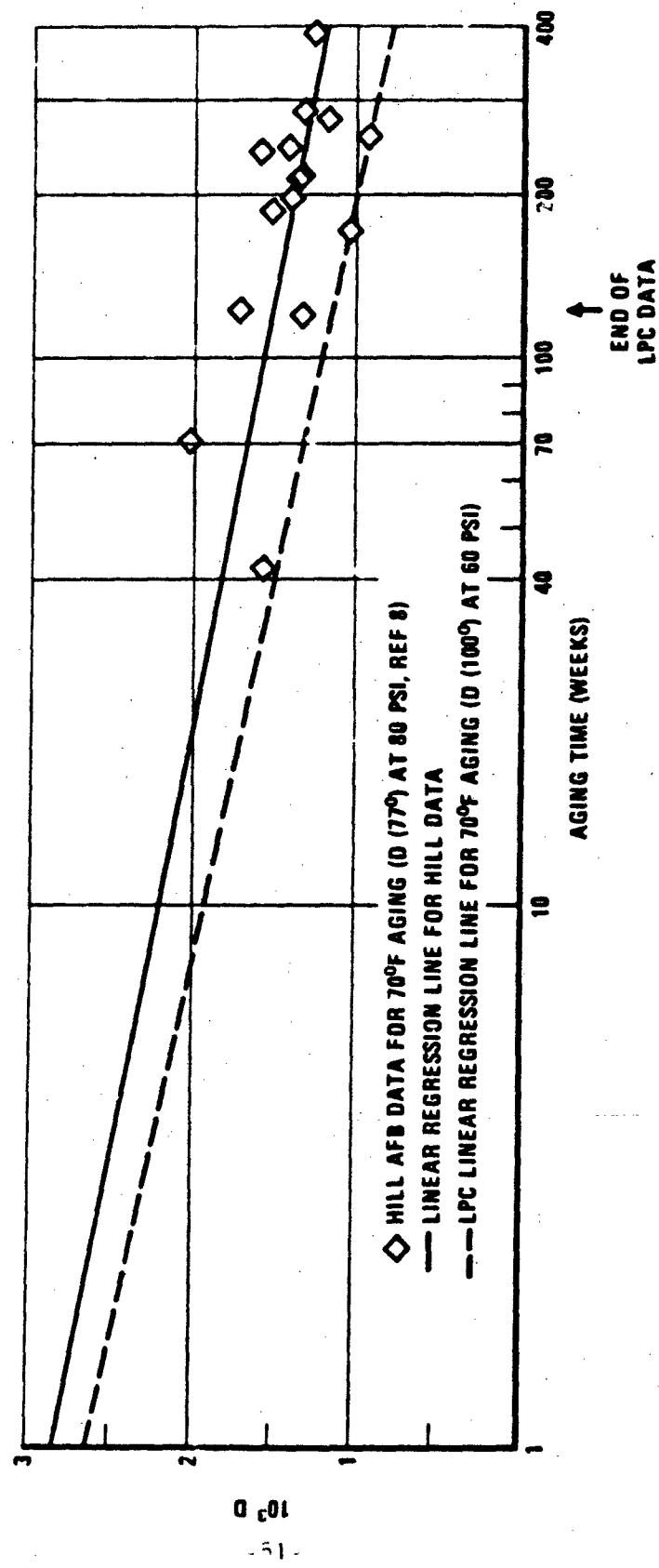
Figure 3-20   Long-Term Aging: Comparison of OOAMA Compliance Data and LPC Prediction

different batches would be required for quantitative clarification.

- Since the use of linear or quadratic expressions in logarithmic time is essentially empirical, other forms obviously could be employed to facilitate time and/or temperature extrapolation, e.g., $f(1/G)$ instead of G when a steady state is achieved and a rapid reversion is known to be absent.

3.2.5 Service Life Prediction

Time extrapolation of the aging regression curves to a predetermined critical value of the particular parameter yields the predicted useful service life of the propellant system. This is demonstrated in Figures 3-21 and 3-22 for D_1 (100^0F) and gel, using only the quadratic regression curves for purposes of illustration. (The vertical, double-ended arrows indicate the $\pm 1\sigma$ limits of the calculated curves at the particular aging times.) The most appropriate failure criterion for third-stage Minuteman is that of allowable strain. This has been converted to a critical D_1 (100^0F) value by multiplying the ratio of allowable strain and the reported average unaged strain for ANB-3066 batches by the unaged D_1 (100^0F) value, i.e., $D_{crit.} = D^0 \times \epsilon_{crit} / \epsilon_m^0$. A critical gel value was approximated in turn using D_{crit} and the empirical G/D correlation given in Figure 3-3.

Table 3-8 summarizes the predicted useful service lives for this batch of ANB-3066 propellant at several storage temperatures and at 0 and 5 percent strain using both the linear and quadratic regression curves. The spread in values at each condition reflects the uncertainty due to the $\pm 1\sigma$ deviations in both the failure criterion and the calculated parameter. In view of the approximations involved in defining the failure criterion, these predicted service lives should be accepted as approximations in terms of their absolute magnitudes, nevertheless the following conclusions or comments are warranted:

- The minimum predicted useful life for this batch at 70^0F is approximately 5 years in an unstrained condition. This is decreased by a factor of about 2 by storage at 5 percent strain, even though the actual rate of aging (log time basis) at 5 percent strain and 70^0F is only slightly greater than at 0 percent strain. Thus even small strains existing in a motor grain may significantly decrease service life and make questionable the predictions made from aging unstrained cartons.

- A strong temperature effect is, of course, observed but it should be noted that initial failure times for compliance/linear log t decrease more sharply with strain than with temperature. Useful life at 60^0F is significantly greater than at 70^0F, particularly under 5-percent strain. In practice, the potential reduction in fleet replacement by storage at 60^0F would have to be considered against the increased cost of maintaining the 60^0F environment.
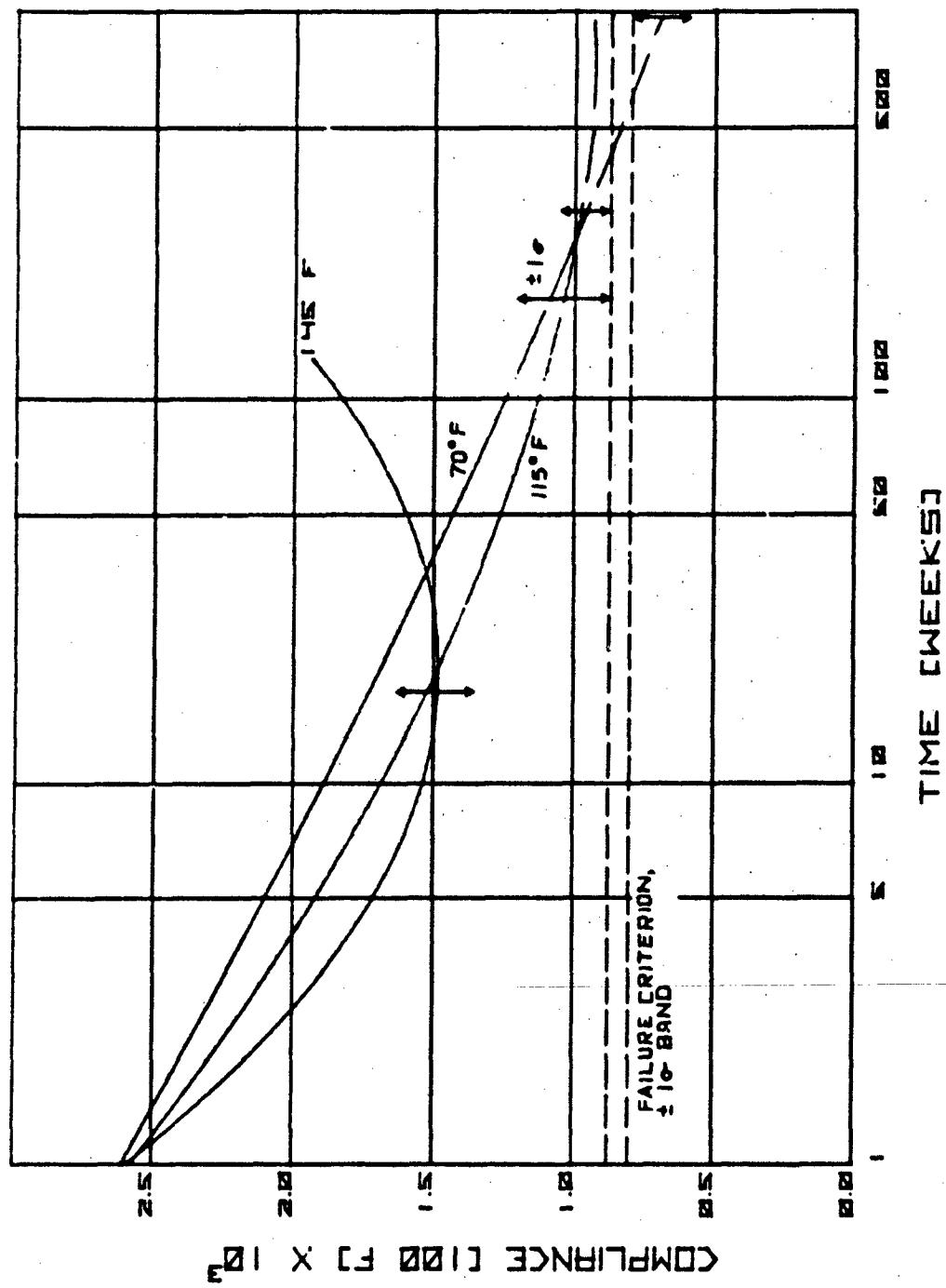
Figure 3-21   Service Life Prediction Using Quadratic Curves For D_1 (100°F)
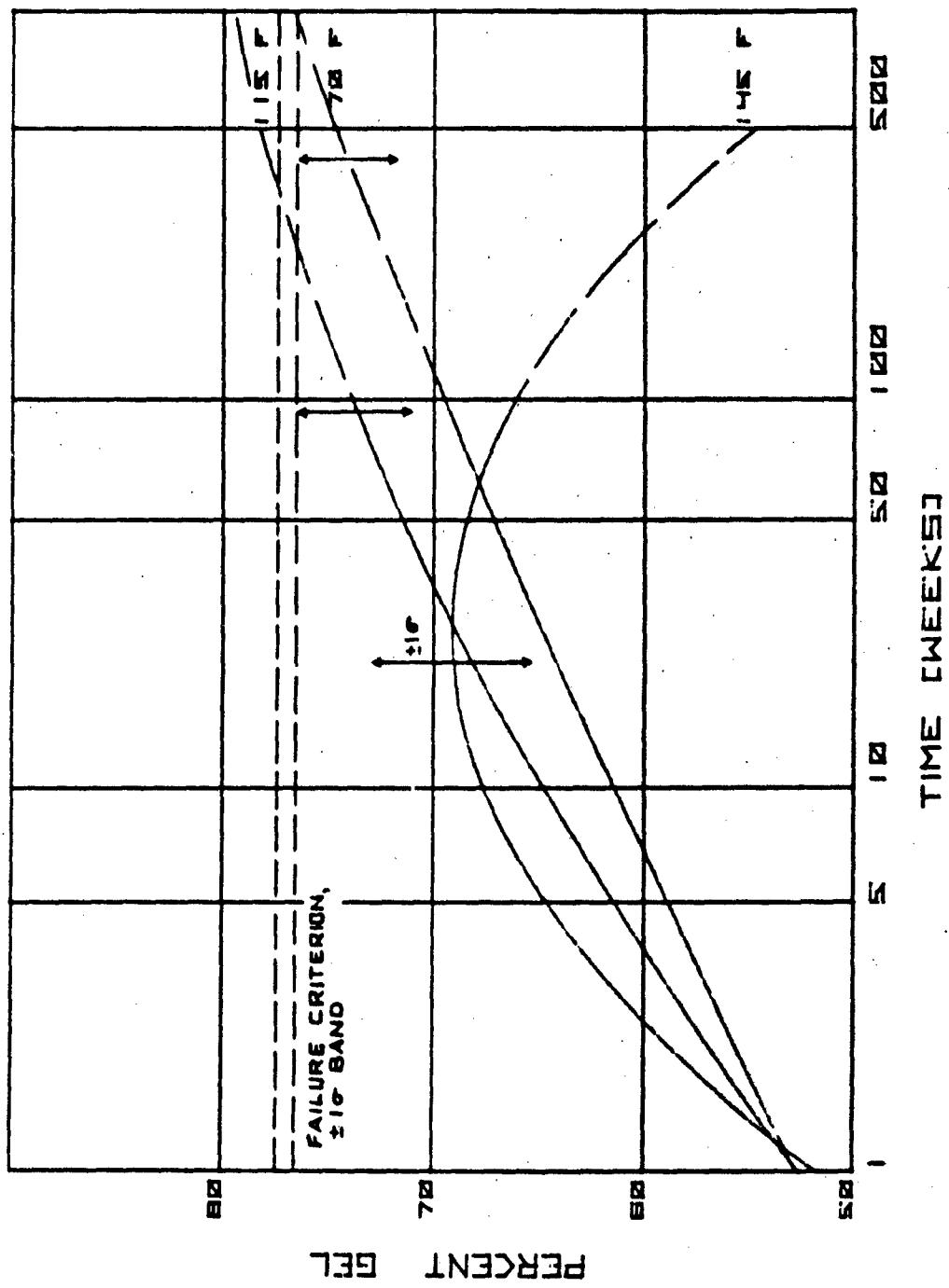
Figure 3-22   Service Life Prediction Using Quadratic Curves For Gel

Table 3-8

SERVICE LIFE PREDICTION FROM CHEMICAL AGING RATES

| Aging Condition | | Predicted Service Life (Years) | | | |
| Temperature (°F) | Strain (%) | From Compliance[1] | | From Gel[2] | |
		Linear Log t	Quadratic Log t	Linear Log t	Quadratic Log t
60	0	6.4 - 18	--	--	--
	5	4.6 - 12	--	--	--
70	0	4.6 - 11	5.8 - 19	7.1 - 29	8.1 - 52
	5	1.7 - 9.2	--	4.8 - 23	--
115	0	1.9 - 8.1	3.5 - (3)	1.4 - 5.8	1.7 - 25
	5	0.3 - 1.0	0.5 - (3)	0.7 - 2.1	-- - (3)
145	0	0.5 - 0.8	--	0.7 - 1.3	-- - (3)
	5	0.2 - 0.4	0.2 - (3)	0.3 - 0.8	-- - (3)

(1) From intersection of ±1σ band for critical D_1 (100°F), i.e., D_1 (100°F) = 0.80 - 0.86, with ±1σ bands for compliance aging curves calculated from rate constants of Table 3-4.

(2) As in (1), using critical gel content (76.4 - 77.3) calculated from critical D_1 (100°F) values and empirical G/D correlation from Figure 3-3.

(3) Does not intersect failure criterion.

- The effect of a reversion process is, of course, to increase the time required to first intersect the failure band and especially to increase the upper time limit. Thus, a mild degree of reversion - or attainment of a steady-state - can be highly desirable, and it is conceivable that longer service life could be achieved by increasing silo temperature rather than decreasing it.

- The desirability of minimizing errors in failure criteria and in expe mental parameters followed during aging becomes obvious from the very large spread in predicted values at any one condition. At 70^0F and 0 percent strain, for example, the uncertainty in useful life is $11-4.6 = 6.4$ years using the linear regression for compliance. If the relative standard deviation of regression is reduced from the observed 3.4 percent for $D_1 (100^0F)$ to 1 percent this spread in predictions becomes $9.6-5.9 = 3.8$ years. Under a more conservative procedure, e.g., one prescribing ±2 or 3 sigma undertainty, this factor naturally becomes magnified and fleet replacement rates would increase rapidly.

4. CONCLUSIONS AND RECOMMENDATIONS

4.1 CONCLUSIONS

The primary conclusion is that the program has met its major goal by demonstrating that accelerated surveillance can indeed be employed to predict chemical aging-controlled service life of ANB-3066 propellant. More specifically, it has been demonstrated that rates of change of propellant physical properties can be quantitatively defined by empirical expressions in logarithmic time and that those rates can be temperature extrapolated using a conventional Arrhenius approach.

The following subsidiary conclusions can also be drawn from the program:

(1) Although the physical properties of ANB-3066 change markedly during aging. this is not accompanied by measurable changes in residual carboxyl or imine concentrations. Instead, it appears that aging changes result from AP oxidative attack upon the polybutadiene backbone.

(2) Distinct batch-to-batch variations in the rate and pattern of aging exist for ANB-3066. particularly at higher temperatures. and this is not corrected by a simple modulus normalization procedure. In addition. the high temperature (145^0F) reversion process indicated with LPC's batch is not strongly evident in available data for several other batches. Therefore. care must be exercised in generalizing quantitative predictions from accelerated data obtained upon one or a few batches.

(3) Chemical aging of ANB-3066 under 5 percent constant strain significantly increases aging rates. especially at higher temperatures. Although the rate increase at 70^0F may be small. its effect upon predicted service life can be large, e.g.. factor of 2 for calculations based upon compliance.

(4) Useful life may be significantly increased by storage at 60^0F. instead of 70^0F. or possibly even by employing temperatures above 70^0F if advantage can be taken of a reversion process.

(5) Examination of the data from this and other propellant aging
programs has identified a number of prerequisites for success-
ful prediction of chemical aging rates by time/temperature
extrapolation:

●   The parameter or properties selected for observation
during the course of aging must be capable of measure-
ment within a relative standard deviation of a few percent.

●   The number of aging points must be as large as budget and
schedule permit. The combined implication of these first
two points is that an aging program should concentrate
upon a small number of critical parameters which are
reproducibly measurable rather than upon screening a
large number of parameters.

●   To ensure meaningful extrapolation, aging should be con-
ducted over a broad temperature range and an extended
time period.

4.2 RECOMMENDATIONS

The above conclusions lead straightforwardly to a number of recom-
mendations:

(1) Analytical methods should still be pursued which are capable
of at least identifying the critical chemical processes respon-
sible for propellant aging and hopefully are capable of
defining their rates quantitatively. Specific attention for
polybutadiene-type propellants should be directed towards
reactions involving the backbone double bonds. Without such
information propellant service life prediction will remain
empirical. In addition, such studies should greatly aid the
development of methods/materials to inhibit the aging processes.

(2) The program has demonstrated that certain empirical methods
of data analysis and extrapolation can be employed for service
life prediction. Future aging programs should examine other
relations and extrapolation procedures as dictated by their
particular data and aging patterns.

(3) The batch-to-batch variations in aging behavior shown by
ANB-3066 provide additional evidence that aging behavior
and service life should constitute important quality control
criteria in propellant manufacture. For that purpose, however,
test techniques for very high accelerated aging would be
desirable.

(4) Consideration should be given to possible cost advantages
accruing from lengthened service life by storage at tempera-
tures other than 70°F.

(5) This program has only just touched upon the interaction
between fatigue and chemical aging. Future programs must
develop a greater understanding of the effects of the mechanical
forces existing in propellant grains upon chemical aging rates
and, in turn, of the effects of chemical aging upon propellant
fatigue resistance. This is particularly important, of course,
for non-silo stored systems where quantitative knowledge of such
interactions may be essential to realistic service life predictions.

(The reverse is blank)

REFERENCES

1. (a) C. B. Henderson, P. H. Graham, C. N. Robinson, Int. J. Fracture Mechanics, 6, 33 (1970)

   (b) W. E. Knauss, G. C. Smith, K. Palaniswamy, CIT, GALCIT SM 73-3, July 1973

2. Aerojet 4158-81F, July 1967, 1143-81F, Oct 1968, 1236-81F, Sept 1969

3. LPC Report 532-F, AFRPL-TR-74-000, October 1974

4. J. Halpin and H. W. Polley, J. Comp. Materials 1, 64 (1967)

5. LPC Report 569-I-1, AFRPL-TR-72-64, June 1972

6. Thiokol, AFRPL-TF-74-16, June 1974

7. Aerojet 0162-026Q-5, Part 1, Aug 1964

8. Aerojet 0162-06 SAAS-11, October 1972

9. MAGCP Report NR 278 (73), October 1973

(The reverse is blank)

Appendix A

EXPERIMENTAL PROCEDURES AND RESULTS

A.1 PROPELLANT PROCESSING, STORAGE, AND PREPARATION FOR TESTING

ANB-3066 propellant was procured as 1-gallon cartons from Thiokol where it was prepared and cured according to Minuteman specifications using Minuteman production facilities (Batch 686-5004). It's initial proper-ties, as measured by Thiokol, were:

E_o 472 psi

σ_m 106 psi

ϵ_m 34%

r_b 0.327 in./sec

Considerable delay was encountered before the propellant was delivered to LPC. The time between end of cure and initiation of aging has been esti-mated as equivalent to 10 weeks at 70^0F.

Figure A-1 illustrates the configuration of ANB-3066 aging blocks, which were wrapped in foil and canned under nitrogen. The original propel-lant cartons were approximately 5 by 7 by 7 inches and were trimmed to the dimensions in Figure A-1 to permit storage in standard 1-gallon cans. For the blocks aged under strain the two 4 by 3-inch faces were bonded to steel plates which were then separated using metal studs/nuts to produce the desired gross strain. After aging, 0.1-inch-thick slices were microtomed from the center portion of the block in the plane perpendicular to the original casting direction, and the direction of straining for those slices as tear, creep, dilatation specimens was kept constant. After removal from the aging cans all blocks and specimens were kept under dry nitrogen except during the brief periods of actual testing.

Propellant was aged at 30, 70, 86, 115, and 145^0F. The purpose of the 30^0F storage was to provide a propellant bank where aging changes would be minimal and from which propellant could be removed and introduced into aging at 70 to 145^0F. In actual practice, it was found that aging occurred at a significant rate at 30^0F, and the means employed to correct the higher tem-perature storage data for varying periods at 30^0F are described in Appendix B.
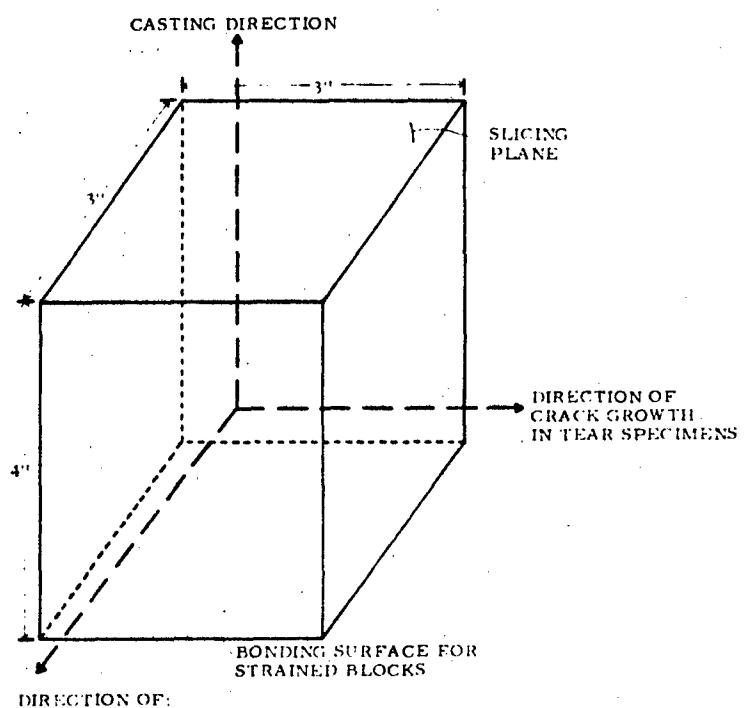
Figure A-1   ANB-3066 Aging Blocks

A.2 GEL CONTENT AND DEGREE OF SWELL

Several of the 0.1-inch-thick propellant slices are cut into $\sim\frac{1}{8}$-inch squares and about 5 g weighed into a wire basket for each of the triplicate samples. The baskets are suspended in toluene vapors for 3 days to allow the major portion of sorption/swelling to occur relatively slowly, then immersed in liquid toluene (50 ml) for a total of 3 days with a change of solvent at the end of the first and second days.*

Each basket is then removed from the solvent, rinsed, blotted against paper toweling briefly, sealed in a tared beaker, and weighed. The beaker caps are removed, the toluene allowed to evaporate at room temperature, and finally the last traces of solvent removed by vacuum.

The degree of swell (S) and the gel content (G) are defined as:

S = grams toluene sorbed/gram gel

G = percent of original <u>polymer</u> plus <u>curative</u> which are insoluble in toluene

The observed gel and swell values are tabulated in Tables A-1 and A-2. The overall relative standard deviations for gel and swell are 1.6 and 3.2 percent, respectively.

A.3 CREEP COMPLIANCE

The apparatus consists of a horizontal platform on which is mounted a fixed metal support and a carriage which travels on two guide rods (Figure A-2). Ball bushings are used to reduce the coefficient of friction of the carriage on the rods to very low values. The carriage is caused to move by known weights suspended by the cable which passes over a block of nylon (the cable is stranded steel covered with nylon). Longitudinal translation of the carriage is detected and recorded by means of the electrical output of a linear variable differential transformer (LVDT). A micrometer is used for the calibration of the LVDT.

A propellant specimen (3 by 1 by 0.1 inch and bonded to wood tabs) is clamped in the position shown in Figure A-2. The output of the LVDT is brought to electrical null and the recorder is started. A known weight is suspended from the weight cable and the displacement of the carriage (and

---

* Preliminary experiments demonstrated that immediate immersion into toluene, i.e., very rapid swelling, led to lower gel contents and higher degrees of swell than measured using an initial vapor phase sorption.

Table A-1

GEL CONTENT FOR ANB-3066[1]

Aging Condition				Aging Condition			
Temperature (°F)	Strain (%)	Time (Weeks)[2]	Gel Content (%)	Temperature (°F)	Strain (%)	Time (Weeks)[2]	Gel Content (%)
30	0	0/30	61.7±1.5	115	0	0/5	61.7±1.5
		35/65	65.0±0.9			3/8	62.3±0.7
		48/78	62.3±0.7			7/19	65.5±0.1
		77/107	65.5±0.8			14/19	71.3±0.4
		91/121	64.5±0.2			14/26	66.±0.6
70	0	0/10	61.7±1.5			22/34	72.2±0.5
		4.5/15	61.8±0.6			40/52	72.3±2.5
		19/29	67.5±0.9			70/82	72.2±0.5
		19/48	64.0±0.3			120/125	74.6±1.0
		40/69	69.6±0.4		5	0/4	61.7±1.5
		58/85	69.0±0.1			3.5/7	63.9±0.6
		86/113	70.6±1.2			7/16	68.5±0.2
		121/131	69.7±0.6			14/18	66.2±3.3
	5	0/8	61.7±1.5			14/21	66.6±0.2
		4.5/13	61.4±1.0			22/29	76.3±0.4
		19/27	68.0±0.2			40/47	76.8±0.5
		19/41	67.7±0.4			71/75	78.9±0.9
		40/62	69.9±0.4			120/124	81.3±0.2
		55/77	71.1±0.6	145	0	0/4	61.7±1.5
		73/93	67.1±0.4			2/6	64.9±0.6
		121/128	70.8±0.5			3/13	67.1±0.2
86	0	0/7	61.7±1.5			10/14	69.4±0.7
		8/29	65.5±0.9			56/61	72.1±3.4
		22/43	68.8±0.8			77/81	57.0±5.4
		36/57	69.1±0.6			88/95	63.0±2.5
		50/71	68.7±0.7		5	0/3	61.7±1.5
		70/87	70.7±0.9			2/5	66.1±0.9
	5	0/6	61.7±1.5			5/12	74.0±2.8
		8/24	67.7±1.0			10/13	68.9±0.8
		22/38	69.5±0.6			121/124	67.0±3.0
		36/52	72.1±1.1				
		52/68	73.5±0.5				
		70/84	70.9±1.2				

[1] In toluene at 75°F
[2] Nominal/corrected

Table A-2

DECREE OF SWELL FOR ANB-3066[1]

Aging Condition			
Temperature (°F)	Strain (%)	Time (Weeks)	Swell
30	0	35/69	14.9±0.3
		48/82	14.0±0.5
		77/111	15.7±0.8
		91/125	14.1±1.1
?	0	0/10	12.4±0.3
		4.5/15	14.5±0.3
		19/29	14.3±0.5
		19/47	14.7±0.2
		40/68	11.7±0.3
		58/84	11.5±0.1
		86/112	11.7±0.3
		121/131	11.4±0.1
	5	0/7	12.4±0.3
		4.5/12	14.0±0.4
		19/26	11.9±0.3
		19/39	13.6±0.2
		40/60	11.4±0.1
		55/75	10.5±0.1
		73/91	12.6±0.4
		120/127	10.6±0.1
86	0	0/7	12.4±0.3
		8/27	12.7±0.3
		22/4:	13.7±0.5
		36/55	11.5±0.7
		50/69	11.4±0.2
		70/85	12.0±0.3
	5	0/5	12.4±0.3
		8/21	12.4±0.2
		22/36	14.2±0.2
		36/50	10.2±0.3
		52/66	9.6±0.0
		70/82	12.4±0.5

Aging Condition			
Temperature (°F)	Strain (%)	Time (Weeks)	Swell
115	0	0/5	12.4±0.3
		3/8	12.9±0.5
		7/18	12.8±0.5
		14/19	10.6±0.2
		14/25	12.2±0.1
		22/33	11.3±0.2
		40/51	10.1±0.5
		70/81	10.4±0.1
		121/146	10.1±0.2
	5	0/3	12.4±0.3
		3.5/7	13.8±0.3
		7/15	12.4±0.2
		14/17	12.1±0.6
		14/22	12.5±0.2
		22/30	10.4±0.3
		40/48	9.4±0.2
		71/74	11.4±0.5
		120/123	9.1±0.1
145	0	0/4	12.4±0.3
		2/5	13.5±0.2
		3/13	10.5±0.3
		10/13	12.1±0.1
		56/64	10.2±0.6
		77/80	16.5±2.2
		88/95	15.1±0.1
	5	0/3	12.4±0.3
		2/5	13.1±0.4
		5/11	9.9±0.4
		10/13	11.5±0.3
		120/123	12.3±0.9

Figure A-2 Creep Measurement Apparatus

thus the elongation of the sample) is detected and recorded with respect to time. Elongations of up to 17 percent (limit of the apparatus) are recorded.

Measurements were performed primarily at -40 and +100°F by enclosing the apparatus in a temperature-controlled box which was located in a low humidity room (< .00 ppm water). A few measurements were made at +75°F and were converted to +100°F using a factor (1.25±0.04) obtained by comparing data for two different samples.

Creep compliance for points in time was calculated according to

$$D = \frac{1}{2.2 \times 10^{-3}} \cdot \frac{AC}{WK\ell_0}$$

where: W = force in grams

K = calibration constant

ℓ_0 = initial specimen length

A = initial cross-sectional area of test specimen

C = chart reading in inches

Compliance values were fit by linear regression to the equation

$$\log D_t = \log D_1 + n\log t$$

using data points from 0.1 to 10 minutes. In this equation t is the time in minutes after loading the sample, D_1 is the compliance value at 1.0 minute, and n is an empirical parameter.

Tables A-3 and A-4 summarize the compliance results as a function of aging condition/time in terms of D_1 and n at +100°F and -40°F, respectively. Data were obtained upon triplicate specimens at 60 psi initial stress. The overall relative standard deviation for D_1 (100°F) is 2.3 percent and for D_1 (-40°F) is 5.8 percent.

A.4   CRACK PROPAGATION

Crack propagation measurements were conducted using 1 by 3 by 0.1-inch propellant specimens bonded to wooden strips along the 3-inch edges and containing an initial 0.5-inch crack at one edge. Measurements were made at 75°F and 0.2 in./in./min strain rate upon triplicate or quadruplicate specimens. By visual observation the point (i.e., stress and strain) at which crack growth initiates was noted, as well as the times required for the crack to grow 0.05, 0.1, 0.15, and 0.2 inch.

Table A-3

COMPLIANCE (100°F) FOR ANB-3066[1]

Aging Conditions				
Temperature (°F)	Strain (%)	Time (Weeks)[2]	$10^3 D_0$ (100°)	n (100°F)
30	0	0/35	1.92±0.07[3]	0.11±0.02
		48/82	1.19±0.04[3]	0.10±0.01
		77/112	1.61±0.02	0.11±0.00
		91/126	1.58±0.04	0.10±0.01
70	0	0/10	1.92±0.07[3]	0.11±0.02
		5/15	1.79±0.06[3]	0.11±0.01
		19/29	1.56±0.05[3]	0.10±0.01
		19/47	1.28±0.02	0.11±0.01
		40/68	1.48±0.09	0.11±0.00
		58/83	1.34±0.01	0.11±0.01
		86/111	1.21±0.01	0.10±0.00
		121/131	1.13±0.00	0.10±0.00
	5	0/8	1.92±0.07[3]	0.11±0.02
		5/12	1.40±0.05[3]	0.11±0.01
		19/27	1.89±0.07[3]	0.07±0.01
		19/40	1.53±0.05	0.09±0.00
		40/61	1.05±0.03	0.09±0.00
		55/61	1.17±0.01	0.09±0.01
		71/92	0.99±0.03	0.09±0.01
		120/128	1.05±0.01	0.10±0.00
86	0	0/7	1.92±0.07[3]	0.11±0.02
		8/27	1.43±0.01	0.09±0.01
		22/41	1.59±0.01	0.10±0.01
		36/55	1.26±0.05	0.09±0.01
		50/69	1.17±0.03	0.10±0.01
		68/87	1.01±0.01	0.10±0.00
	5	0/5	1.92±0.07[3]	0.11±0.02
		8/22	1.37±0.00	0.08±0.01
		22/36	1.41±0.02	0.08±0.00
		36/50	0.95±0.02	0.09±0.00
		52/66	0.88±0.02	0.10±0.01
		68/82	1.06±0.04	0.09±0.01

Aging Conditions				
Temperature (°F)	Strain (%)	Time (Weeks)[2]	$10^3 D_0$ (100°)	n (100°F)
115	0	0/5	1.92±0.02[3]	0.11±0.02
		3/8	1.79±0.06[3]	0.14±0.00
		7/18	1.56±0.06	0.11±0.05
		14/19	2.02±0.07[3]	0.07±0.01
		14/25	1.32±0.04	0.11±0.00
		22/33	1.19±0.03	0.10±0.01
		40/51	1.43±0.03	0.10±0.00
		70/81	1.42±0.04	0.09±0.00
		121/126	0.87±0.00	0.10±0.01
	5	0/3	1.92±0.02[3]	0.11±0.02
		3/7	1.42±0.05[3]	0.10±0.01
		7/15	1.15±0.01	0.10±0.01
		14/17	1.00±0.03[3]	0.12±0.01
		14/22	1.23±0.12	0.09±0.00
		22/30	0.86±0.00	0.09±0.00
		40/48	0.86±0.04	0.10±0.01
		68/76	1.02±0.02	0.09±0.01
		120/123	0.61±0.01	0.10±0.01
145	0	0/3	1.92±0.02[3]	0.11±0.02
		2/5	1.64±0.06[3]	0.10±0.01
		3/12	1.49±0.04	0.10±0.00
		10/13	1.62±0.06[3]	0.11±0.01
		56/63	1.56±0.03	0.10±0.00
		77/80	3.57±0.58	0.17±0.02
		87/94	1.90±0.03	0.08±0.00
	5	0/2	1.92±0.02[3]	0.11±0.02
		2/4	1.23±0.04[3]	0.10±0.01
		5/10	1.01±0.03	0.09±0.00
		10/12	1.06±0.04[3]	0.09±0.01

(1) Data points from 0.1 to 10 minutes fitted to $D(t) = D_1 t^n$ where D_1 is creep compliance at one minute. Measured at 60 psi initial stress on 2 to 3 specimens.

(2) Nominal corrected.

(3) Corrected from value measured at 75°F. Correction factor of 1.25±0.04 determined from two different cartons.

Table A-4

COMPLIANCE (-40°F) FOR ANB-3066[1]

Aging Condition				
Temperature (°F)	Strain (%)	Time (Weeks)	$10^4 D_1$ (-40°F)	n (-40°F)
30	0	48/73	1.90±0.25	0.17±0.02
		77/103	1.24±0.04	0.18±0.01
		91/117	1.55±0.13	0.17±0.02
70	0	0/31	1.90±0.25	0.17±0.02
		19/50	1.41±0.01	0.17±0.01
		40/71	1.28±0.24	0.18±0.02
		55/86	1.39±0.04	0.18±0.02
		86/114	1.34±0.18	0.14±0.02
		121/131	1.37±0.16	0.13±0.03
	5	0/30	1.90±0.25	0.17±0.02
		19/49	1.96±0.13	0.17±0.00
		40/70	0.94±0.10	0.16±0.01
		55/85	1.24±0.19	0.13±0.02
		73/101	1.25±0.10	0.14±0.01
		121/130	1.28±0.03	0.4±0.01
86	0	0/22	1.90±0.25	0.17±0.02
		8/31	1.04±0.04	0.23±0.03
		22/45	1.82±0.16	0.17±0.02
		36/59	1.21±0.14	0.16±0.02
		50/73	0.74±0.07	0.13±0.06
		70/91	1.18±0.06	0.14±0.00
	5	0/19	1.90±0.25	0.17±0.02
		8/27	1.41±0.13	0.18±0.01
		22/42	1.77±0.14	0.15±0.01
		36/56	0.85±0.23	0.17±0.08
		52/72	0.67±0.14	0.15±0.00
		70/88	1.30±0.01	0.13±0.01

Aging Condition				
Temperature (°F)	Strain (%)	Time (Weeks)	$10^4 D_1$ (-40°F)	n (-40°F)
115	0	0/12	1.90±0.25	0.17±0.02
		7/21	1.25±0.05	0.19±0.01
		14/28	1.27±0.01	0.15±0.01
		22/36	1.18±0.01	0.14±0.02
		40/54	1.23±0.08	0.15±0.01
		70/83	0.84±0.16	0.16±0.03
		120/126	1.13±0.09	0.10±0.02
	5	0/10	1.90±0.25	0.17±0.02
		7/17	1.41±0.13	0.18±0.01
		14/24	1.23±0.04	0.14±0.00
		22/32	1.27±0.06	0.12±0.01
		40/50	0.38±0.11	0.16±0.04
		73/78	1.23±0.12	0.12±0.03
		120/124	0.96±0.09	0.11±0.01
145	0	0/10	1.90±0.25	0.17±0.02
		3/15	1.03±0.24	0.19±0.02
		56/65	1.30±0.11	0.18±0.02
		77/81	1.98±0.22	0.18±0.01
		88/96	1.44±0.08	0.19±0.01
	5	0/7	1.90±0.25	0.17±0.02
		5/12	0.83±0.11	0.14±0.06

[1] See Table A-3 footnotes.

Table A-5 summarizes the results in terms of the stress (σ_c) and strain (ϵ_c) at growth initiation, the fracture energy ($\gamma_c \cong 0.1875 \; \sigma_c \cdot \epsilon_c$), and the growth rate for the first and second 0.1 inch. The reported errors are one sigma, and the overall relative standard deviations are 22 percent for γ_c, 12 percent for σ_c, 9 percent for ϵ_c, and ~20 percent for growth rate.

A.5 DILATATION

Samples for dilatation were milled from the interior of aging blocks into specimens 0.4 by 0.4 by 3 inches, bonded at the ends to wooden tabs, the long (straining) dimension being perpendicular to the original casting direction, and parallel to the strain direction in the case of propellant blocks aged under 5-percent strain.

Volumetric dilatation of these uniaxial specimens was obtained by making simultaneous measurements of the axial and lateral strains while under load in an Instron at $75^0 F$ and 0.02 in./in./min strain rate. Figure A-3 illustrates the strain gage device employed in measuring the lateral strain.

Measurements were taken until the specimen failed at the propellant-wood bond, i.e., >10 percent strain. For convenience the data are reported as percent dilatation, $\Delta V/V$, at the 8-percent strain level. Triplicate specimens were used and the errors reported in Table A-6 represent the 1σ values. The overall relative standard deviation of $\Delta V/V$ (8 percent strain) is 14 percent.

Table A-5

FRACTURE PROPAGATION FOR ANB-3066[1]

Aging Condition						Rate of Crack Growth (in./min)	
Temperature (°F)	Strain (%)	Time (Weeks)[2]	σ_c	ϵ_c	γ_c	0.5 to 0.6 in.	0.6 to 0.7 in.
30	0	48/63	66±11	7.8±1.3	0.99±0.31	0.65±0.13	0.80±0.13
		77/93	84±11	7.4±0.9	1.2 ±0.3	0.46±0.06	0.98±0.20
		91/107	68±1	7.6±0.5	0.97±0.07	0.52±0.07	0.94±0.14
70	0	0/35	66±11	7.8±1.3	0.99±0.31	0.65±0.13	0.80±0.13
		19/56	84±12	6.9±0.9	1.1 ±0.3	0.68±0.06	1.04±0.01
		40/59	67±8	7.9±0.5	0.99±0.16	0.53±0.04	0.99±0.22
		58/87	77±10	7.3±0.5	1.1 ±0.2	0.53±0.04	1.04±0.10
		86/115	80±8	7.5±0.7	1.1 ±0.2	0.87±0.21	1.10±0.15
		120/131	82±12	7.4±0.6	1.2 ±0.3	0.77±0.12	1.20±0.33
	5	0/35	66±11	7.8±1.3	0.99±0.31	0.65±0.13	0.80±0.13
		19/54	75±2	7.3±0.2	1.0 ±0.1	0.50±0.01	1.16±0.16
		40/75	81±7	7.7±0.8	1.2 ±0.2	0.60±0.11	0.96±0.22
		55/90	93±15	9.3±1.2	1.7 ±0.5	0.62±0.10	0.87±0.12
		70/106	91±5	7.7±0.6	1.3 ±0.2	0.65±0.05	1.04±0.16
		120/130	93±6	6.8±0.8	1.2 ±0.2	0.86±0.06	1.23±0.08
86	0	0/29	66±11	7.8±1.3	0.99±0.31	0.65±0.13	0.80±0.13
		8/39	82±4	7.1±0.4	1.1 ±0.1	0.69±0.12	0.91±0.14
		22/53	65±4	6.5±0.4	0.80±0.10	0.48±0.07	0.94±0.12
		36/67	74±9	7.0±0.4	0.98±0.18	0.74±0.15	1.04±0.24
		50/81	92±5	7.4±0.4	1.3 ±0.1	0.61±0.10	1.01±0.09
		70/99	72±12	6.4±0.4	0.86±0.20	0.87±0.45	1.03±0.11
	5	0/29	66±11	7.8±1.3	0.99±0.31	0.65±0.13	0.80±0.13
		8/39	72±8	6.7±0.4	0.91±0.15	0.69±0.04	1.06±0.17
		22/53	88±10	7.7±0.8	1.3 ±0.3	0.49±0.13	1.09±0.37
		36/67	89±6	7.1±0.5	1.2 ±0.1	0.70±0.08	1.15±0.17
		51/83	104±12	8.6±0.9	1.7 ±0.4	0.99±0.31	1.14±0.13
		70/99	75±11	7.5±0.9	1.1 ±0.3	0.71±0.07	1.03±0.16
115	0	0/22	66±11	7.8±1.3	0.99±0.31	0.65±0.13	0.80±0.13
		7/30	60±12	5.6±1.4	0.66±0.29	0.56±0.04	1.08±0.23
		14/37	89±2	7.7±0.4	1.3 ±0.1	0.69±0.13	1.08±0.14
		22/45	73±16	6.2±1.1	0.88±0.34	0.50±0.12	0.79±0.21
		40/63	76±6	6.4±0.9	0.92±0.19	0.72±0.07	1.41±0.23
		70/89	96±13	10.0±1.2	1.8 ±0.4	0.44±0.02	0.55±0.08
		121/128	68±9	5.2±0.6	0.61±0.20	1.56±0.46	1.79±0.19
	5	0/22	66±11	7.8±1.3	0.99±0.31	0.65±0.13	0.80±0.13
		7/30	82±12	8.1±1.1	1.3 ±0.4	0.83±0.21	0.94±0.27
		14/37	78±8	6.1±0.1	1.0 ±0.4	0.91±0.21	1.22±0.33
		22/45	72±7	6.1±0.1	0.82±0.09	0.70±0.08	1.04±0.04
		40/63	95±11	6.0±0.5	1.1 ±0.2	0.88±0.17	1.18±0.17
		70/91	88±10	6.9±0.9	1.2 ±0.3	0.82±0.10	1.04±0.24
145	0	0/18	66±11	7.8±1.3	0.99±0.3	0.65±0.13	0.80±0.13
		3/28	87±1	9.5±0.4	1.5 ±0.1	0.50±0.02	0.66±0.11
		56/71	84±2	7.3±0.9	1.2 ±0.2	0.58±0.03	0.84±0.09
		88/102	67±3	8.9±0.9	1.1 ±0.1	0.48±0.05	0.68±0.09

[1] At 75°F and 0.2 in./in./min on 1 x 3 x 0.1 in. strips with initial 0.5 inch edge cut. Triplicate or quadruplicate specimens.

[2] Nominal/corrected from σ_c analysis.

PROPELLANT
SPECIMEN

0.010 IN.
SPRING STEEL

2 SEMI-
CONDUCTOR
STRAIN GAGES

1.5 IN.

0.4 IN.

0.25 IN. WIDE
SPRING STEEL

PROPELLANT, 0.375
TO 0.40 IN. SQUARE

PLEXIGLASS
SUPPORT
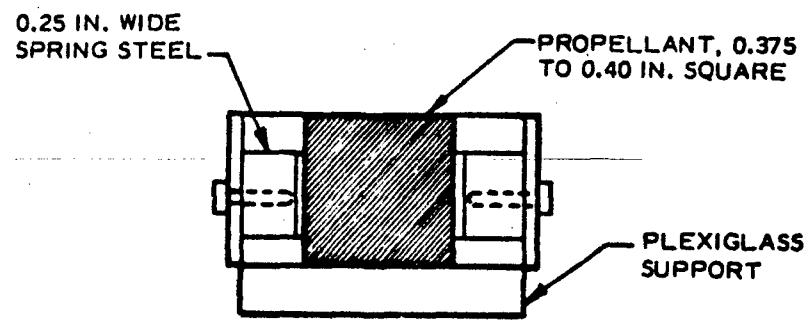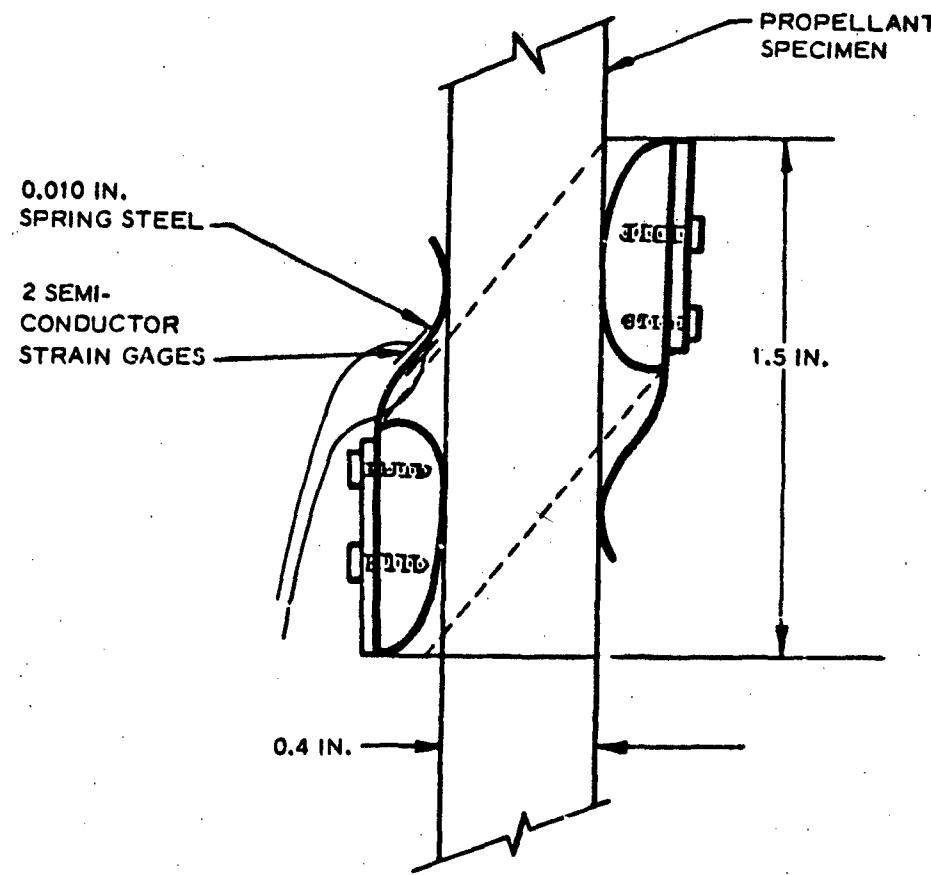
Figure A-3   Schematic of Lateral Strain
Measuring Device

-74-

Table A-6

DILATATION OF ANB-3066[1]

Aging Condition				Aging Condition			
Temperature (°F)	Strain (%)	Time (Weeks)[2]	ΔV/V at 8% Strain (%)	Temperature (°F)	Strain (%)	Time (Weeks)[2]	ΔV/V at 8% Strain (%)
30	0	48/61	3.6±1.0	115	0	0/30	3.6±1.0
		77/91	2.8			7/37	2.1±1.4
		91/105	1.3±0.3			14/44	0.7
70	0	0/46	3.6±1.0			22/52	2.0±0.2
		19/65	3.5±0.4			40/70	0.6±0.1
		40/86	0.1±0.1			70/96	2.5±0.1
		58/97	1.4±0.3			121/129	1.1±0.3
		86/125	1.4±0.3		5	0/30	3.6±1.0
		121/131	0.9±0.2			7/37	2.2±0.5
	5	0/46	3.6±1.0			14/44	3.1±0.4
		19/65	2.4±1.0			22/52	3.8±0.2
		40/86	1.5±0.1			40/70	2.0±1.2
		55/97	1.0±0.3			73/96	3.0±0.6
		73/125	1.1±0.2	145	0	0/25	3.6±1.0
		121/135	2.2±0.1			3/38	1.4±0.6
86	0	0/39	3.6±1.0			56/61	1.0±0.1
		8/50	2.3±0.1			87/109	0
		22/64	0.9±0.6				
		36/78	1.9±0.1				
		50/92	2.0±0.1				
		70/110	2.4±0.3				
	5	0/39	3.6±1.0				
		8/50	1.7±0.1				
		22/64	2.7±0.3				
		36/78	2.3±0.5				
		52/92	2.3±0.7				
		70/110	2.1±0.5				

(1) Measured at 75°F and 0.02 in./in./min

(2) Nominal/corrected

(The reverse is blank)

Appendix B

PROCEDURE FOR KINETIC DATA ANALYSIS

The following iterative procedure was employed to fit the parameter aging data to equations (B-1) and (B-2)

$$P = P^0 + k \log t \qquad (B-1)$$

$$P = P^0 + k_1 \log t + k_2 (\log t)^2 \qquad (B-2)$$

(1) Gel content was selected as the primary parameter since it appeared to be the most reliable measurement and more data points were available. All other parameters were plotted against gel content to establish a self-consistent set of initial estimates for the various P^0's.

(2) For each parameter, regression analyses were performed against equations (B-1) and (B-2) using the experimental values plus the above P^0 and the nominal aging times. This resulted in a new estimate for P^0, obtained by averaging the P^0 values produced by the regression at each temperature. It further provided an initial estimate for relative aging rates.

(3) Using the above aging rates (k values), initial corrections to the nominal aging times were made. For example, in the simple case of correcting the aging time at some temperature T for the initial 10-week period at 70^0F,

$$\Delta P_{70^0} = k_{70} \log 10 = \Delta P_T = k_T \log \delta t_T.$$

(4) Regression analyses were repeated with the corrected P^0 and corrected aging times, leading to more accurate values of P^0, k's, and aging times. Further iterations were performed until changes in P^0 and k's were slight and little significant improvement was observed in the standard deviation of regression.

(The reverse is blank)

Appendix C

EXPLANATIONS FOR BATCH VARIATIONS IN
AGING BEHAVIOR

There are several factors that can be expected to alter the aging rate
and pattern among different batches and not be accounted for by simply
normalizing the data according to initial (unaged) moduli. Figures C-1 and
C-2 illustrate two such effects for cure and aging at a single temperature,
using Thiokol gel content data as a baseline.

Figure C-1 illustrates the effect of differences in cure chemistry in
terms of the effective availability of curative, e.g., through differences in
initial stoichiometry or differences in aziridine conversion to oxazoline. An
important general point to be noted first is that cured propellants, being
lightly crosslinked, are only just beyond the region of steeply rising gel and
crosslink density - and therefore mechanical integrity. Consequently,
rather small decreases in extent of reaction may have major effects upon
propellant structure and properties, as illustrated schematically in
Figure C-1.

At high effective curative availability the structural build-up will be
initially rapid but the rate probably will drop off more rapidly than it does
in the intermediate case due to earlier restrictions upon molecular mobility.
Assuming the same aging mechanism in the two cases, the upper curve more
quickly achieves the long-term aging rate. At low curative availability
structural buildup will be delayed but once gel begins to form the rate will
still be rapid. Again assuming the same aging mechanism, the initial aging
rate will be more rapid because the system is still in the highly sensitive
gel/extent of reaction region. Eventually the aging rate will approach the
same long-term values exhibited by the initially more highly crosslinked
batches.

Figure C-2 illustrates the extremes in apparent aging behavior that
might be expected due to the broad modulus acceptance limits for ANB-3066,
assuming identical cure and aging chemistry. Suppose that batches identical
in all respects to that represented by the solid line were removed from cure
when they attained a modulus (and gel content) represented by the lower and
upper specification limits. If these were then placed in "aging" at the same
temperature, their "aging" behavior would appear to follow the two dashed
lines.

In actual practice, batch-to-batch variations may involve combinations
of the effects described above plus perhaps other differences in aging
mechanism or rate. Small differences in effective stoichiometry, for
example, may be randomly – or deliberately – combined with small changes
in cure schedule. The result will almost certainly be effectively different
rates and patterns of aging, those differences being most evident during the
early aging period.
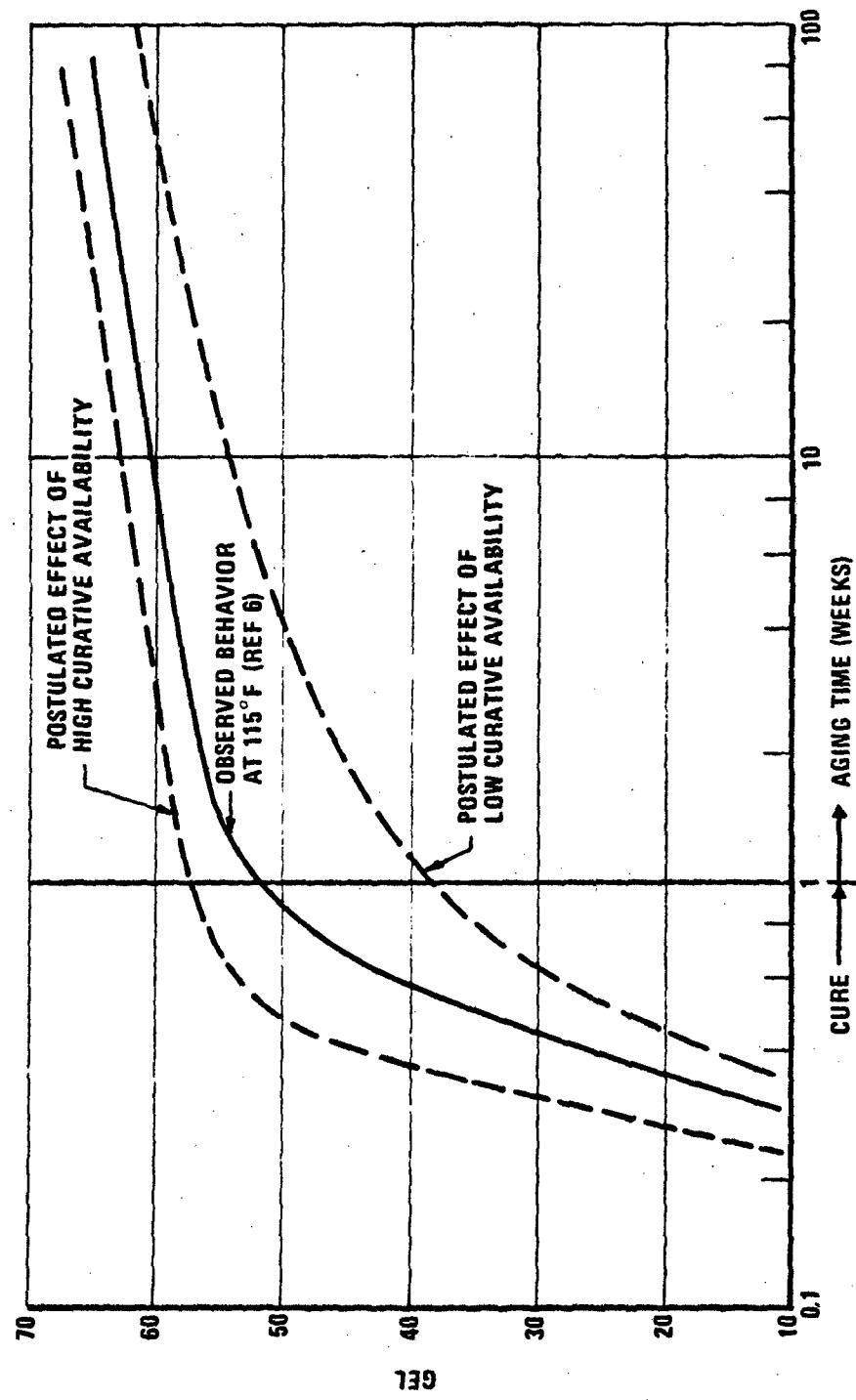
Figure C-1   Effect of Changing Cure Chemistry Upon Rates of Cure and Aging
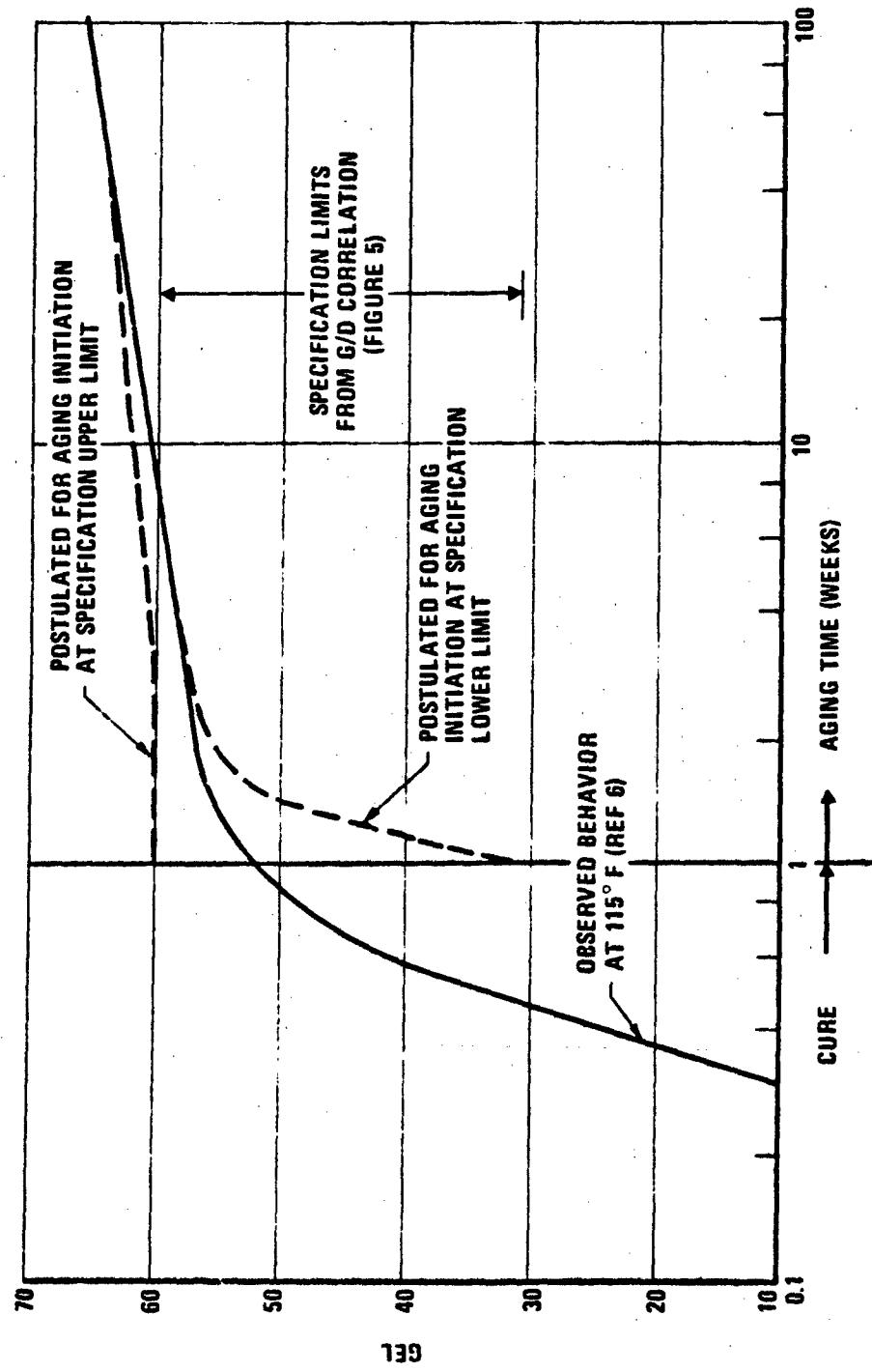
Figure C-2   Possible Influence of Specification Range Upon Apparent Aging Behavior, Assuming No Changes in Cure Chemistry

There appear to be two ways to obviate, or at least minimize, these effects in order to improve the reliability of service life predictions and of fleet replacement rates. The first is to tighten control procedures with regard to stoichiometry, mix cycle, cure cycle and to tighten property acceptance limits. The second is to introduce into the quality control requirements the measurement of gel content or modulus upon at least occasional batches during cure and an initial aging period; such data could constitute an invaluable acceptance criterion in terms of both unaged properties and service life.

GLOSSARY

B	Apparent activation energy
D_1 (100°F)	Compliance measurement at 100°F one minute after load application
D_1 (-40°F)	As above, at -40°F
G	Gel content
GPC	Gel permeation chromatography
k	Aging rate constant for linear log time dependence
k_1, k_2	Aging rate constants for quadratic log time dependence
LPC	Lockheed Propulsion Company
MIR	Multiple internal reflectance infrared
n	Slope of compliance equation, $\log D = \log D_1 + n \log t$
S	Swell
s	Standard deviation
$\Delta V/V$	Dilatation in % at 8% strain
γ_c	Fracture energy
ϵ_c	Strain at crack growth initiation
σ_c	Stress at crack growth initiation

(The reverse is blank)